1-31-2012

Multi-mission radar waveform design via a distributed SPEA2 genetic algorithm

Brent Josefiak

Multi-Mission Radar Waveform Design via a Distributed SPEA2 Genetic Algorithm

by

Brent Josefiak

A Graduate Thesis Submitted

in

Partial Fulfillment

of the

Requirements for the Degree of

MASTER OF SCIENCE

in

Electrical Engineering

Approved by:

_____

(Dr. Vincent Amuso, Graduate Advisor)

_____

(Dr. Sohail Dianat, Committee Member)

_____

(Dr. Ferat Sahin, Committee Member)

_____

(Dr. Sohail Dianat, Department Head)

January 31, 2012

DEPARTMENT OF ELECTRICAL AND MICROELECTRONIC ENGINEERING

KATE GLEASON COLLEGE OF ENGINEERING

Contents

Acknowledgements

My loving wife Tara who has kindly dealt with and encouraged me along the path to completing my Master's work. Without your amazing support I would not have been able to finish, thank you!

I have to give immense thanks to my family for their over the years. Mom and Dad thank you for all you've sacrificed to provide me with the best possible opportunities, I appreciate them every day and must credit it with so much of my success.

So many of my coworkers at Harris RF who have answered questions and help reinforce the value of the education I was pursuing. The supervisors, especially Glen and Jeff who helped work with me when classes fell at inopportune times and helped me balance success at work with completing my education.

Dr. Amuso, for the tremendous opportunity to continue work on the this project and guiding me forward. Your insights and tutelage made this whole endeavor possible and very rewarding for me to work on.

Abstract

This thesis furthers the development of Genetic Algorithms (GAs) and their application to the design of multi-mission radar waveforms. An application was developed with the goal of developing a waveform suite that finds the Pareto optimal solutions to a multi-objective optimization radar problem. Utilizing the Strength Pareto Evolutionary Algorithm 2 (SPEA2) a series of radar parameters are optimized along the fitness metrics of interest. This implementation builds upon the previous work to develop an application that is capable of analyzing longer more realistic scenarios by using a distributed grid computer to spread the computational load across multiple CPUs. It also advances the previous research by solving for the Pareto optimal front of a simultaneous Synthetic Aperture Radar (SAR) and Moving Target Indication (MTI) mission. These results are presented to validate the performance of the new distributed application against previous work and introduce results of larger more realistic scenarios for a multi-mission radar suite.

Previous Work

This initial work of this thesis was presented at the 2012 International Waveform Diversity & Design Conference. "A Distributed Object-Oriented Multi-Mission Radar Waveform Design Implementation" written by Dr. Vincent Amuso and Brent Josefiak and was presented by Dr. Amuso

1. Introduction

Waveform diversity seeks to optimize the performance of a radar system by tailoring the operating parameters to suit a particular mission and spectral allocation. Many radar systems have been shown capable of performing multiple missions, such as SAR and MTI, but they cannot do them simultaneously [2]. Designing a waveform capable of adequately performing multiple missions simultaneously would offer significant advantages in cost and risk. However, this design problem is non-trivial as it requires a solution that balances complementary and competing design parameters.

There are various techniques available to solve the multiple objective problem proposed by a multi-mission radar waveform, but evolutionary computing has proven an effective tool [2]. Genetic algorithms, with their ability to correlate waveform mission parameters to generic fitness metrics, offer a way to effectively search a radar waveform's multi-dimensional solution space. Previous work in this area created a waveform design suite capable of proving that the Strength Pareto Evolutionary Algorithm 2 (SPEA2) could effectively optimize both SAR and MTI missions [1]. The suite encoded radar parameters, such as center frequency, azimuth angle and number of pulses per coherent pulse interval, as genetic information, would be used to run through a scenario and measure its fitness. Mission performance was measured across different objective functions for the SAR and MTI scenarios, but these were then mapped to the generic fitness values used by SPEA2.

The initial work done in this area proved its feasibility, but the implementation was limited in scalability and could not complete larger scenarios. Bringing more computational capacity to bear on this problem would allow for multi-second scenarios that would be directly applicable to real-world applications. To this end, the SPEA2 multi-mission radar suite was rewritten as a C++ application that could be run on a Linux based multi-core grid computer. The significant number of two dimensional Inverse Fast Fourier Transforms required to measure the performance of a SAR waveform can gain significant speed boosts when run in the parallel grid environment.

This paper proposes the continued application of SPEA2 to the multi-mission radar problem, but by utilizing a more computationally efficient and extensible framework. This new implementation will be examined in detail to explain how some of the design trade-offs were chosen and how to best refine it into a more powerful waveform design suite. The performance of

the new C++ radar suite will be validated by reconstructing the SAR and MTI scenarios described in "SPEA2 applied to simultaneous multi-mission waveform design" [1]. Optimizations to the algorithm's implementation will allow for scenarios that simulate a larger SAR mission with higher resolution PSL and ISL.

The performance gained by utilizing the Message Passing Interface (MPI) to parallelize the processing of population members will also be examined. This was the primary speed-up that allowed for a combined large scale MTI and SAR mission to be examined.

2. C++ Class Implementation and Functionality

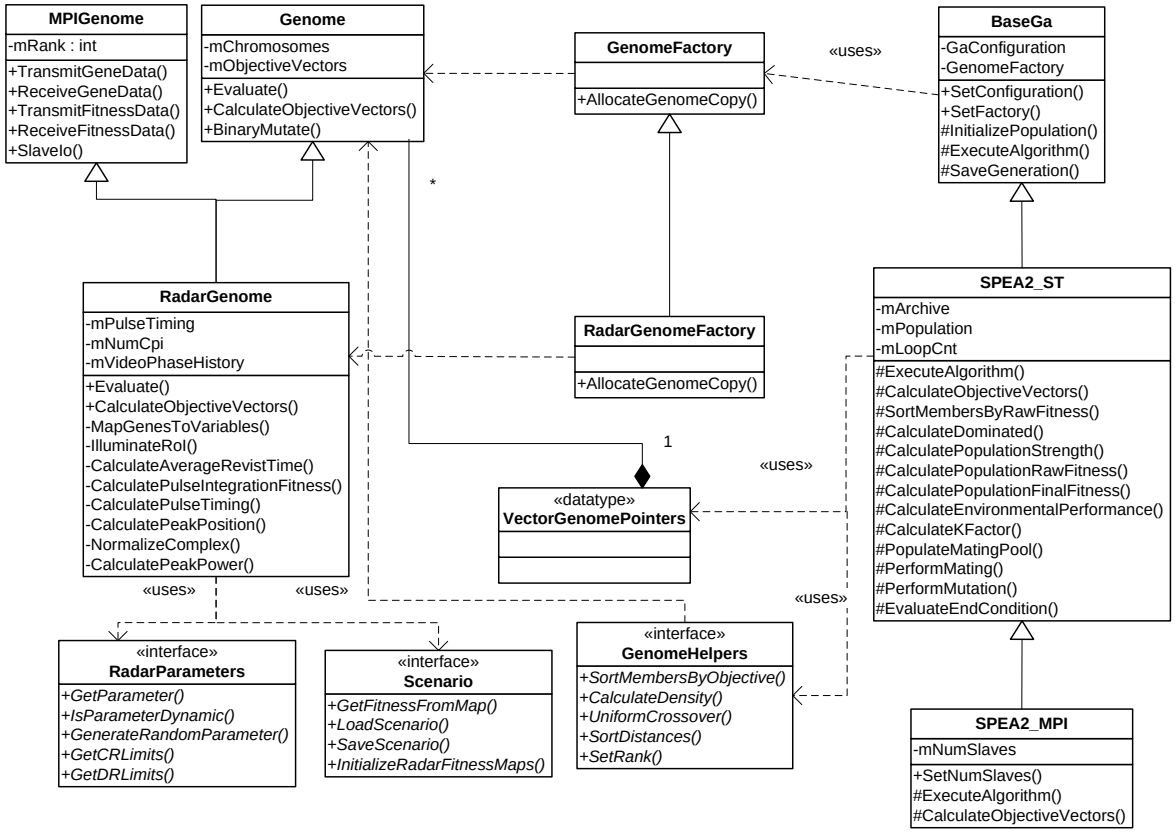

Figure 1 C++ Radar Waveform Design Suite Class Diagram

Figure 1 is a UML diagram laying out the relationship between the Genetic Algorithm, its population members (Genomes) and the helper functionality supporting them. At the lowest level, there are the Genome and BaseGa classes[14]. The specific algorithm implementations, such as SPEA2, which inherit from the BaseGa, will contain populations of Genomes to act

upon. The Genome class contains the genetic information required for a given problem, but not the ability to interpret the encoded information; that task is left to a derived class.

New population members are constructed through a GenomeFactory class, which isolates the algorithm from the problem specific genome implementation.[14] This factory is provided to the algorithm as part of the initialization. Radar data and functions are contained in the RadarGenome class that is derived from the base Genome. The radar members contain the ability to translate their generic genetic information into radar specific parameters (azimuth angle, center frequency, etc).

The GenomeHelper interface provides a layer of abstraction that manipulates the inner workings of multiple genomes. This prevents the genetic algorithm from needing to understand the inner workings of its genomes when it desires operations involving two or more genomes. An excellent example of this is uniform crossover, where the algorithm provides the helper with two genomes and, based on the scenario's crossover probability (provided as part of the scenario initialization), the helper function handles the swap of genetic information. The other helper functions in this class fall into this category of acting upon two or more genomes.

SPEA2_ST is the single threaded SPEA2 implementation derived from the BaseGa, which implements and validates the original waveform design suite algorithm in C++. The SPEA2 implementation acts upon two genome sets, the new member population and archive pools. It contains the functionality required to calculate the raw fitness, strength and final ranking of the populations.

SPEA2_MPI is the MPI compatible implementation of SPEA2, which re-implements the algorithm to distribute genetic information from the master algorithm to a set of slave genomes. These slaves are distributed across multiple cores so that the computationally intensive 2D IFFTs required to calculate PSL and ISL can be run in parallel. When the current set of slave genomes have yielded their fitness data, 0.0 to 1.0 values representing the success of that particular member, it is transmitted back to the master. The master process then continues to calculate the remainder of the algorithm as if the fitness had been calculated locally.

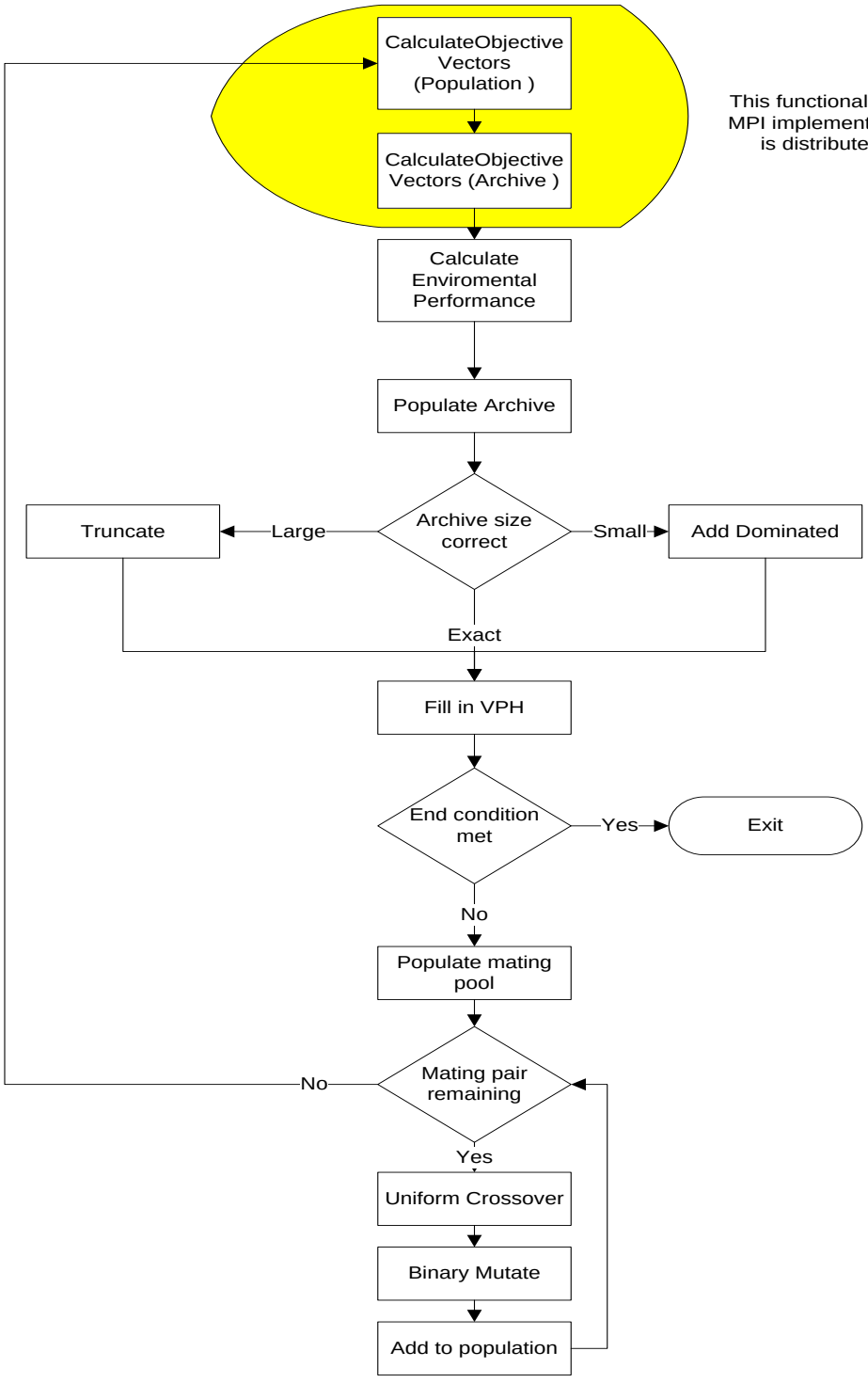

Figure 2 SPEA2 ExecuteAlgorithm

Figure 2 and 3 highlight the changes to the Execute Algorithm and Calculate Objective Vectors functions that were overridden from the original single threaded implementation. Calculate Objective Vectors now distributes the members of both the archive and new population

pools off to the genome slaves. The total number of slaves is configurable at run-time and can utilize as many cores as are available on a given grid implementation.

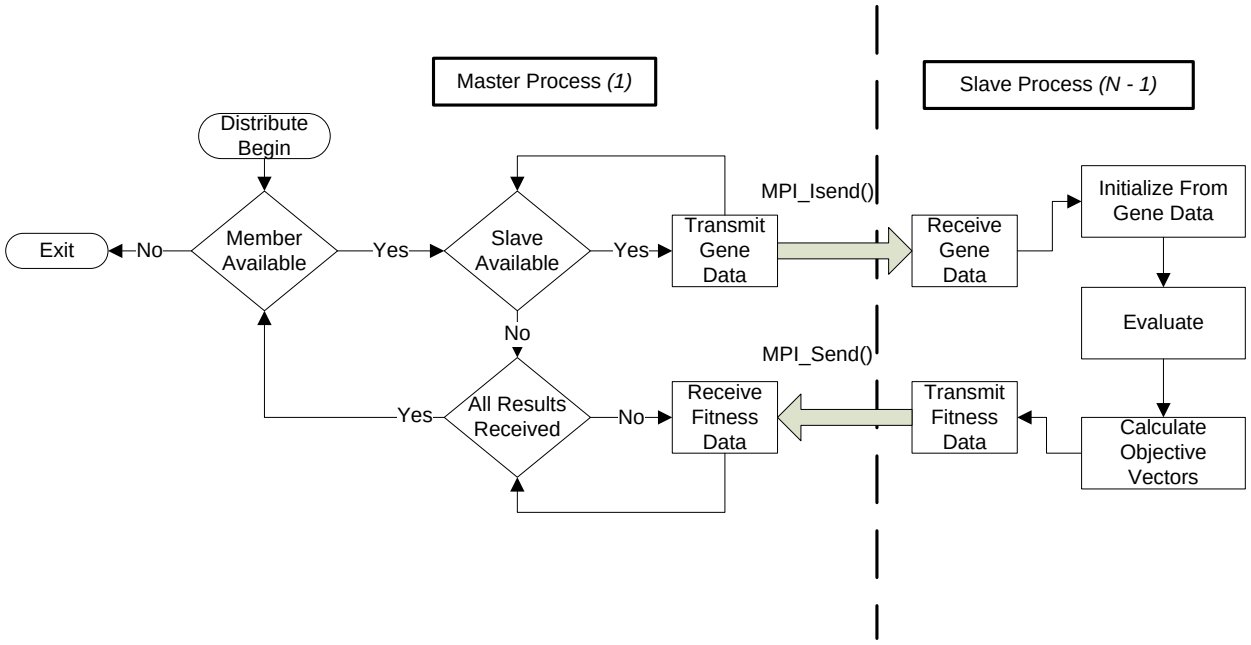

Figure 3 MPI Calculate Objective Vectors - Parallel Computation Distribution and Result Recovery

For a population of size *Np* and archive of size *Na*, an optimal number of processors would be $Np + Na + 1 = Copt$. This allocates a core for every population member and one for the master algorithm. The current software suite will not yield any benefit when there are more cores available than combined population and archive members. See sections 6 and 7 for a detailed analysis of the MPI performance improvement.

It should be noted that two different MPI transmission mechanisms are used when transmitting gene data verses the returning slave generated fitness data. When the master is distributing information to the various tasks it utilizes MPI_Isend, which is the non-blocking send. As each slave process is known to be waiting at this point, the master can send the information to each immediately without waiting for an acknowledgement back. This readiness can be assured because synchronization occurs when the slave process calls MPI_Send (the blocking call) to return the fitness data. As soon as the slave has returned its fitness data, it is available to begin processing a new set of genetic information.

3. Scenario and Algorithm Configuration

A run of the test suite requires two files for configuration parameters, one that sets the general genetic algorithm parameters and one to configure the scenario specific radar parameters. These parameters are stored in human readable text files that are provided as arguments when the program is launched. General configuration information required by the BaseGa is listed in Table 1, along with the description of each parameter.

Table 1 Base GA Configuration Format

Parameter	Description
numPopulation	Number of members in the Population
numArchive	Number of members in the Archive
maxGenCnt	Maximum number of generations to iterate
numFitness	Number of fitness vectors
numMating	Number of member pairs in the mating pool
crossoverProbability	Probability determining location of uniform crossover
mutationProbability	Probability of a bit in the genetic information flipping
saveName	File name to pre-pend to save information
savePath	File save path
numGenPerSave	How many generations to skip between saves

Radar scenario parameterization is defined in a second file and loaded into a dynamic parameter map during runtime initialization. This map allows each RadarGenome access to the scenario configuration by indexing based on the requested parameter. If a parameter is dynamic for a given scenario, it will contain all the potential values index-able by the genetic information of a population member.

The first parameter in the scenario file is the random number seed. Saving the seed allows a scenario to be reproduced again in the future. Given the same random seed value, a run of the algorithm will produce identical results, as all of the randomness in the algorithm is based on the pseudorandom "randn" functionality. Changing this value is necessary to examine how different populations would respond to the same scenario.

Next in the scenario file is the total simulation time. This straightforward parameter

determines the length in seconds the scenario will model. Taken with Pulse Repetition Frequency (PRF) and pulses per interval, this value determines the number of Coherent Pulse Intervals (CPI) a waveform will transmit.

The next line in the configuration file currently contains 4 bits, which toggle the various fitness metrics on and off. In order, these bits enable (1) or disable (0) the use of the Peak Side Lobe (PSL), Integrated Side Lobe (ISL), Average Revisit Time and Integrated Pulses fitness functions. Any combination of these can be can be used, but the total number of enabled fitness functions must match the number provided to the base genetic algorithm. Failure to match these parameters will cause the GA to use the first *n* fitness vectors, where *n* is the number specified within the GA's configuration file.

The lines after this are the 22 configuration parameters that describe a radar scenario. Each line is a comma delimited string and contains a digit stating which parameter it is (0 -21), next a digit stating whether it's an integer (0) or double (1) parameter, then the number of values that parameter can assume, and finally the values themselves. Each parameter can assume between 1 and 2^{32} possible values in steps of powers of 2. If only one value is provided, the parameter is considered static and not included in the genetic information of population members.

Parameters for the CPI (enumeration 0), Number of Apertures (enumeration 1), PRF (enumeration 6) and the total simulation time are used to determine the length of the genetic information of a given member. When any of these parameters are dynamic, and thus contained in the genetic information, the number of alleles used by population members will vary. When a population member is initially generated, all the dynamic parameters of a given CPI are randomized and it is pushed onto a vector. After each CPI is generated, the time elapsed is checked, the number of pulses divided by the selected PRF, to ensure it does not exceed the total simulation time. If the number of apertures is dynamic, the other dynamic parameters are repeated *A* times for a given CPI, where *A* is the number of active independently steerable apertures. Despite the repetition of all dynamic parameters, each CPI in a multiple aperture scenario can only select one PRF and number of CPIs (if these parameters are dynamic). This limits the multiple apertures to mainly altering the steering parameters.

The remainder of the parameters laid out in the scenario configuration file focus on defining the ROI, the target platform and the VPH processing that will occur. The target

platform is the plane carrying the radar waveform, and its movement is defined as a line along the ROI cross range at a speed specified by parameter 14 in meters per second. The perpendicular distance from the ROI is defined in meters by parameter 17.

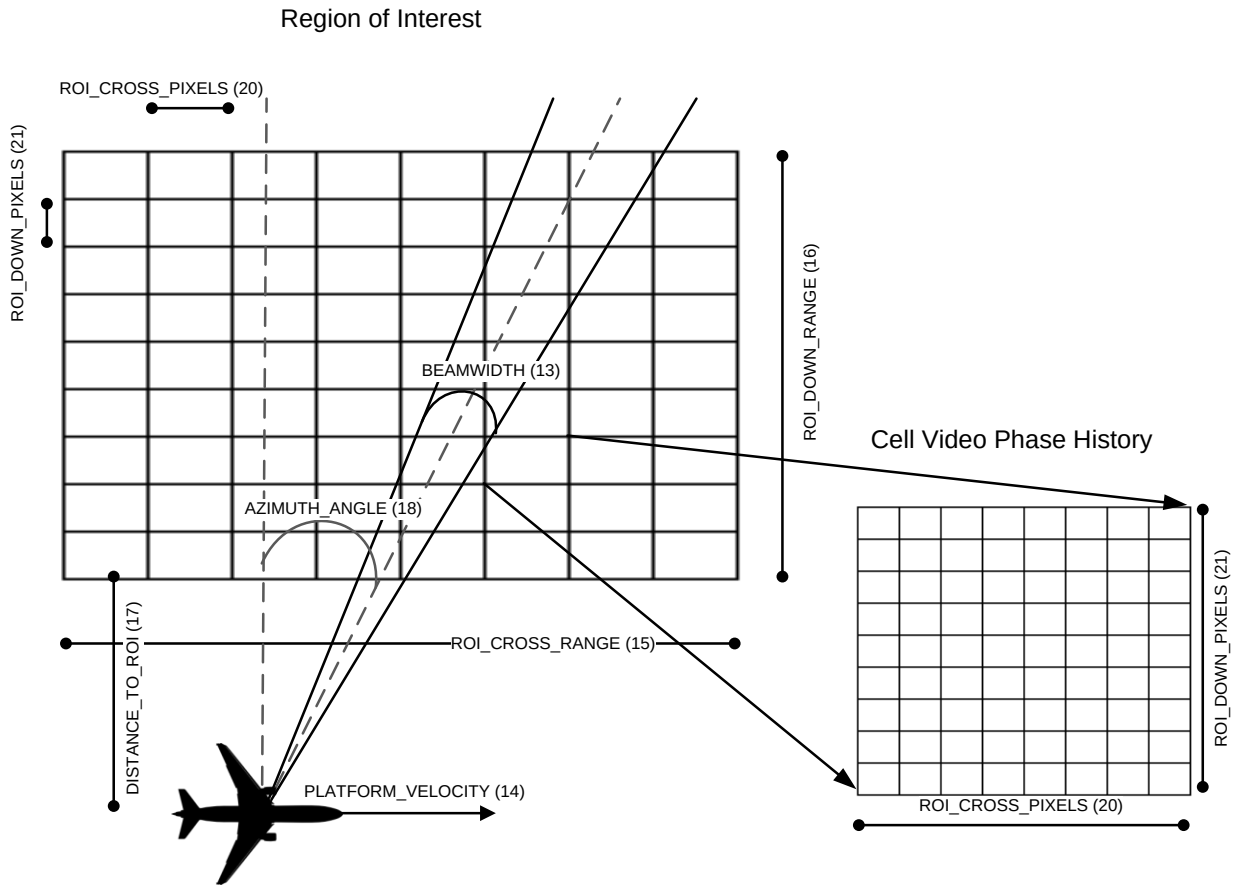

Figure 4 Scenario Parameter Representation

The other scenario parameters highlighted in Figure 4 are the ROI region parameters, which define the total cross and down range (15/16) in meters, as well as the size of a pixel within that region (20/21). Each one of these cells is made up of a VPH array of size defined by parameters 20 and 21, typically 128 x 128. The final parameter required for the computation of PSL and ISL are the IFFT cross and down-range dimensions, which define the resolution and complexity of the 2D - IFFT calculation.

4. Fitness Mapping

Other than the two configuration files defining algorithm and scenario parameters, there are files that define the behavior of the fitness maps. Four fitness map files are used to define the

mapping between a scenario specific parameter and the 0.0-1.0 fitness metric used by the SPEA2 algorithm. Currently there are two formats for these files, which is stated in the first line of the file; 0 for an integer based mapping and 1 for a floating point implementation. After the type is determined, the next line tells how many data points the file contains and the maximum value possible for the objective value. Each of the subsequent lines then lists an objective value (in either integer or double format) and its corresponding fitness value. When the radar member maps an objective to fitness value, if it does not match one of the points provided in the map, it takes the linear interpolation between the two closest objective values to determine the correct fitness value.

4.1. **Genetic Representation**

Each base genome contains all the genetic information required for a given scenario and, once the member has been evaluated, its performance data. Base genetic information is stored in an array of 32-bit values. Each 32-bit allele will be used by the problem specific (RadarGenome) class to map to a scenario relevant value. These alleles are capable of mapping up to 2^{32} different parameters, should the functionality be desired, but most parameters are kept to around 5-bits or 32 values. The one restriction on parameter mapping in the current implementation is that the scenario must use 2^N mappings exactly (where N is 0-32)*;* non power of 2 mappings results in an invalid configuration. This constraint was placed to prevent mutation from generating an allele without a valid parameter mapping.

4.2. **Uniform Crossover Operator**

Uniform crossover is applied to each mating pair selected for the new population pool. The crossover point is selected based on the smaller parent genome and the crossover probability, which is typically 0.5, so that any location is equally likely to be the crossover location[2]. A check for the smaller parent is required for situations when pulse per CPI or PRF are dynamic and can alter the total number of genes present in a given population member. Valid crossover points must be on allele boundaries, but are not constrained by where a CPI or aperture boundary may lie.

4.3. **Binary Mutation Operator**

The binary mutation operator works based on a probability of flipping provided by the configuration file and the number of bits per allele defined in the scenario configuration. After the members of the mating pool have undergone uniform crossover, each is subjected to mutation. This mutation operator iterates over each bit in the population member's genetic information; then a random number is generated and checked against the range defined by the GA's mutation probability. If the value is in the specified percentage of the random range, then the bit is flipped by XORing the current allele with a 1 shifted to location of the current target bit.

4.4. **Radar Genome Mapping**

The Radar Genome takes each allele to be an index into the scenario's dynamic parameter map. The total number of alleles in a given member must be a multiple of the number of dynamic parameters in a given radar scenario.

$$\text{size(CPI)} = \frac{\text{size(Alleles)}}{\text{size(Dynamic Parameters)} * \text{size(Apertures)}}$$

The radar member class uses the static scenario parameters as well as the dynamic values mapped to its genetic information to construct a coherent pulse interval timing sequence. This sequence defines at what position the target platform initiates a given CPI, where it is aimed, and how many pulses are triggered at a given PRF, which defines at what platform location and times a waveform burst will be triggered.

5. **Radar Scenario Calculation**.

Once this burst information is constructed, the platform location and antenna steering parameters are used to determine which cells of the region of interest (ROI) are illuminated in a given coherent pulse interval (CPI). This information is stored in a 2 dimensional Pixel Illumination Vector where each ROI cell has a vector that is pushed back with new pulse timing each time it is illuminated. After it is known which bursts illuminate a given ROI cell, the Video Phase History (VPH) can be filled in, and the MTI revisit time parameter can be calculated [1].

To illuminate the VPH, two factors come into play. The cross range VPH cells are illuminated based on the pulse time, number of pulses and PRF, while the down range is based

on the bandwidth and number of apertures. As highlighted in Figure 4, the VPH dimensions are defined by the down and cross pixel count. When a single aperture is used, the down range, or column as seen in Figure 5, is fully illuminated. Multiple apertures cause the down range dimension (rows) to be divided up so that the bandwidth is allocated evenly amongst sub-apertures as seen in Figure 6. The cross range illumination is determined by the following equations:

$$CR_{start} = \frac{T_{pulse} * NumCRPixels}{T_{sim}}$$

$$CR_{\Delta} = \frac{NumPulses}{PRF} * \frac{NumCRPixels}{T_{sim}}$$

$$CR_{End} = CR_{start} + CR_{\Delta}$$

Where T_{sim} is the total simulation time and $T_{pulse}$is the time a given CPI begins to illuminate the ROI. The CR_{start} and CR_{End} variables are used to index into the VPH and determine which cross range (columns) are illuminated by the current CPI, as can be seen in Figure (x, y).

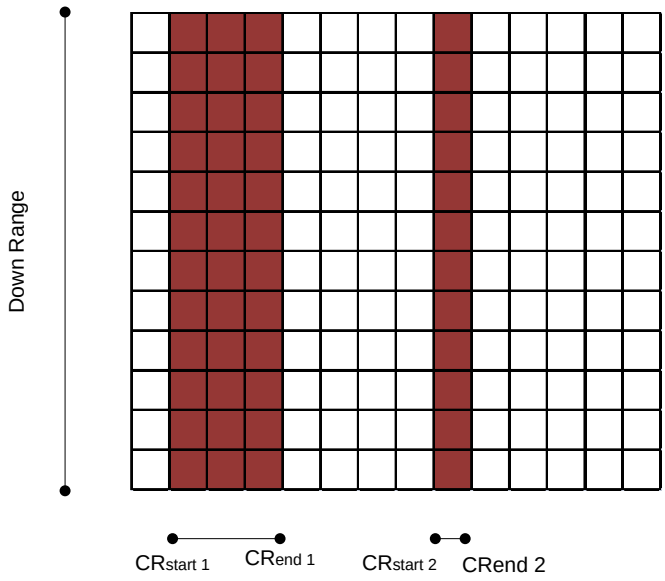

Figure 5. Single Aperture Illumination.

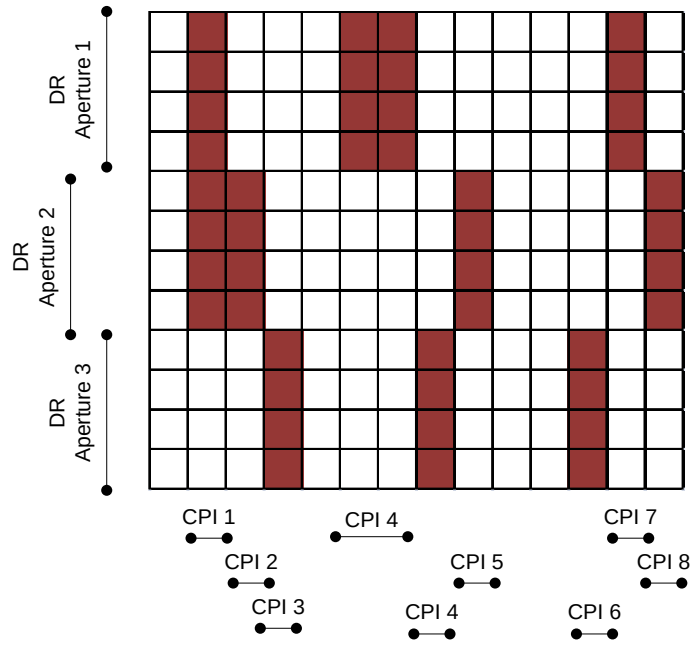

Figure 6. Multiple Sub-Aperture Illumination.

One may notice that we are iterating across all the CPI's twice in the algorithm shown in Figure 7, unfortunately memory limitations on the size of the VPH limited the number that could be allocated. The smaller scenario, where a 256x256 2D-IFFT is computed, necessitated 256(DR) * 256(CR) * 8(Bytes per double) * 2 (complex) = 1 MB of contiguous memory per VPH buffer, two of which are required per ROI cell (one for input and one for output). Although several could be allocated, not enough were available to provide one for every ROI cell, so we are forced to iterate over the CPI two times.

Once all the CPIs that illuminate a given ROI cell have illuminated it, the 2-dimensional IFFT can be run across the VPH. The 2-dimensional Inverse FFT is calculated using the FFTW library developed by Matteo Frigo and Steven Johnson of MIT. This library is upheld by benchmarks as the fastest available FFT implementation and is licensed for use in Matlab. The IFFT dimension is typically twice that of the VPH pixel count so that there is sufficient resolution to calculate PSL and ISL. Were further computing power available, increasing this resolution would be an area to invest it.

The complex information generated by this operation is normalized to a power mapping, which is then used to find the PSL and ISL performance. In order to calculate PSL and ISL, the main power lobe is located and the total power contained within it is summed. The remainder of the power mapping is then summed in order to calculate the ISL. While iterating across the remaining pixels, the maximum value found is saved and used to calculate the PSL.

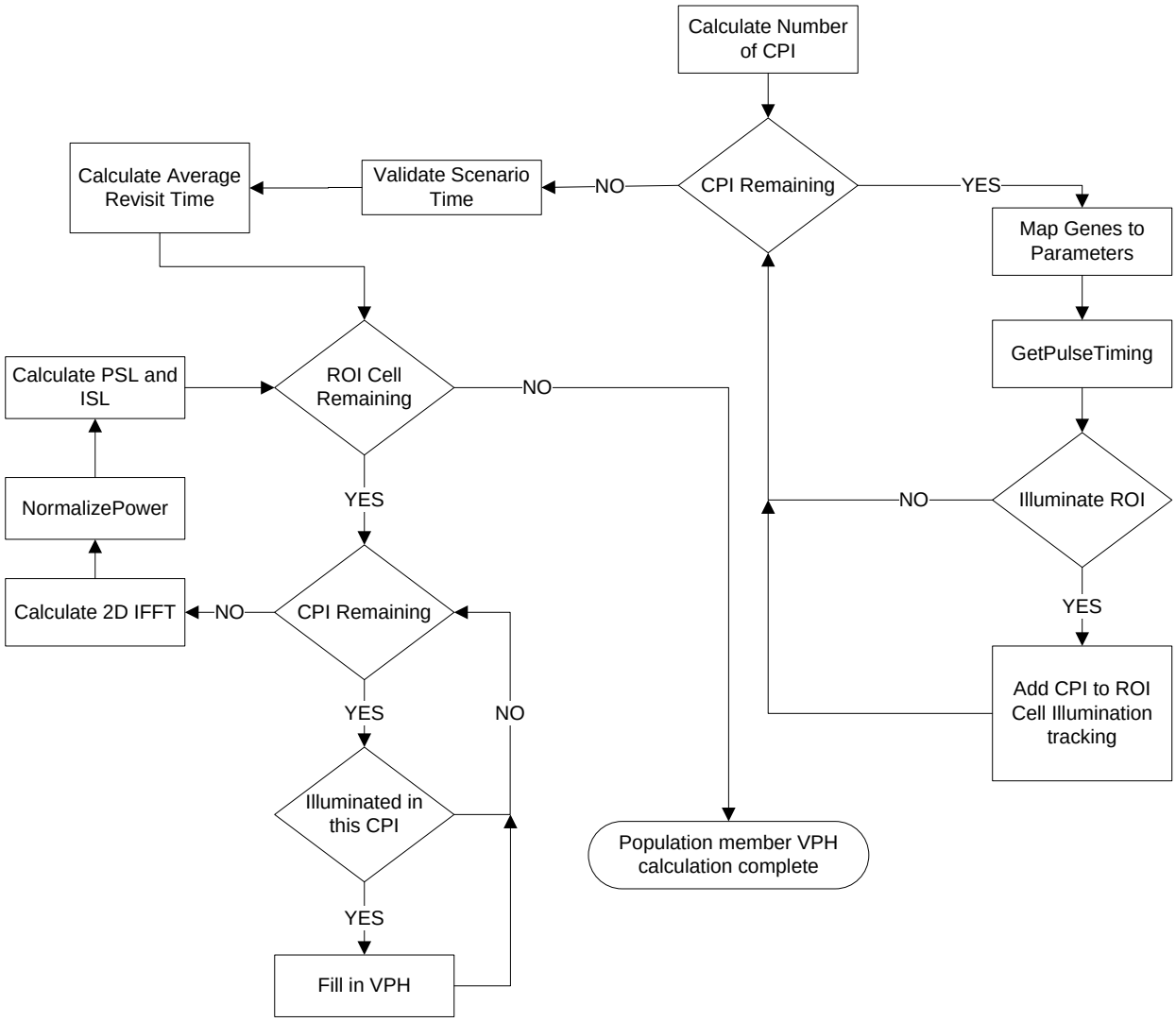

Figure 7. Radar Genome Evaluation

Once the radar calculations have been completed the performance data is gathered. These values are then used to index a fitness map, which normalizes performance into a fitness value between 0.0 and 1.0; this value is then accessed by the SPEA2 algorithm to rank the

performance of population members. In the case of the MPI implementation it is this normalized fitness value that is returned to the master. Further detail on how SPEA2 uses this fitness information to select the fittest members for addition to the archive can be found in [3].

6. MPI Performance Validation

Just as the initial C++ implementation was validated against the original Matlab implementation, so too was the grid implementation validated against previous results. The resulting genetic algorithm performance, once differences in CPU performance were normalized, were in line with the expected parallelization gains. The MPI grid used for the simulations presented later in this paper had only had 30 cores available, while most test runs contained a population size of 100 and archive size of 20. This is well below the *Copt* found previously, so it becomes important to understand the distribution scheme and its affect on parallelization.

When testing began on the grid one immediate revelation was that running a single threaded implementation was slower than an identical run to generate the single threaded results of previous C++ simulations. This was caused by a CPU difference and the difference was baselined by running a series of 256 by 256 2D-IFFT. A single grid core was capable of executing this in 10ms, which is 3x slower than the previous implementation. Despite this silicon setback the "embarrassingly parallel" nature of the genetic algorithm scenario allowed the other 27 cores to prove the value in a distributed algorithm.

As noted previously, information is distributed to the slaves in batches based on how many slaves have been constructed. This batch scheduling approach means that a speed-up only occurs as slaves increase by least common multiples of the total population size.

$$batch\ count = \left\lfloor \frac{size(population)}{(Ncores - 1)} \right\rfloor$$

Thus the total speed up versus the single threaded implementation is given by:

$$speed\ improvement = \frac{Calculation\ Time\ (SingleThread) * size(population)}{Calculation\ Time\ (MPI) * batch\ count}$$

7. MPI Grid FFT Performance

In order to understand the time required to compute the 2D-IFFTs of a generation, a testbench was written. This test suite randomly illuminates a VPH and tracks the time required

to compute its IFFT averaged over a hundred runs. The results from these runs can be seen in the following Table 2.

Table 2. IFFT Time

VPH CR	IFFT2 CR	Time Per Transform (sec)	Time Per Member - 45m x 1000m (sec)	Time Per Member - 45m x 1000m (min)
128	256	0.0198682	66.161106	1.1026851
256	512	0.04555384	151.6942872	2.52823812
512	1024	0.11810853	393.3014049	6.555023415
1024	2048	0.26291108	875.4938964	14.59156494
2048	4096	0.56116136	1868.667329	31.14445548

These test runs were all computed with a VPH down range dimension of 128 and IFFT down range 256. The cross range dimension was repeatedly doubled from an initial IFFT of 256 up to 4096. One can see that the 128 x 256 transform required 0.0198 seconds to complete, while the 2048 x 4096 required 0.5611 seconds per calculation.

The large 45m by 1000m ROI scenario requires each member to calculate 3330 2D-IFFTs, yielding the time required per member found in columns 4 and 5. Using the equation generated in the previous section, one can determine that running a population size of 120 (20 archive plus 100 mating population), at the 256 by 512 size would require 51 minutes per generation in pure FFT calculations.

When running the later SAR scenarios, this theoretical number was proven to be correct with each generation requiring 55-56 minutes to complete. A full real-life SAR mission would require the 45m by 1000m scenario to run with a VPH cross range of at least 2048 to provide a column to each CPI pulse. Calculating this scenario with the current grid would require 622.88 minutes per member, or over 10 hours per generation.

8. SAR C++ Validation

The C++ SPEA2 waveform suite was first validated against the original SAR mission. In this scenario, a platform illuminates a 45m by 30m region of interest in a 0.346 second run. The original fitness mappings for PSL and ISL to the 0.0 to 1.0 fitness value were reused by the C++ implementation. Table 2 lists all the relevant parameters including the dynamic azimuth angle, which is encoded in the genetic material of each population member. Running this scenario has yielded the following results which are in line with the initial work found in [2].

Figure 8 is the Illuminated VPH for the center cell of an archive member of the randomly generated initial population. Note its relatively sparse illumination – only a small number of the waveform's CPIs were landing within the ROI. Contrast this with Figure 9 and one can see how the 350 generations have found genetic material, which better illuminates the ROI cell. This yields a significant improvement in PSL and ISL.

The improvement in fitness performance is illustrated in Figure 10. Over the course of 350 generations, the PSL and ISL have both improved by 6-7dB, which results in a fitness improvement of 0.3-0.4. The fitness improvement of SPEA2 in this mission is not linear as most of the growth occurs within the first 50 generations, while the remaining 300 offer a fraction of growth. Understanding when fitness improvement tapers off allows for testing scenarios to an optimal generation count and once this has been reached a new scenario can be tested more quickly.

Table 3. SAR Parameters

Simulation Parameters	**Value**
No. of Apertures	1
Physical Aperture size	12λ m
Effective aperture length	45 m
Center frequency	600 MHz
Bandwidth	50 MHz
PRF	369 Hz
No. of pulses	1
VPH dimensions	128 x 128
IFFT size	256 x 256
Cross range resolution	3 m
Down range resolution	3 m
Beamwidth	5°
Platform Velocity	130 m/s
Region of Interest Cross Range size	30 m
Region of Interest Down Range size	45 m
Distance to Region of Interest	500 m
Azimuth angle	-30°to30°in 32 steps
Objective Functions	PSL & ISL
Crossover Operator Uniform	50%
Mutation Operator Binary	5%

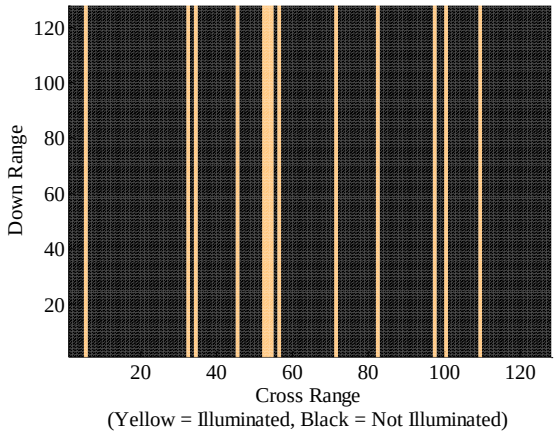

Figure 8. Initial VPH for the center cell of the ROI.

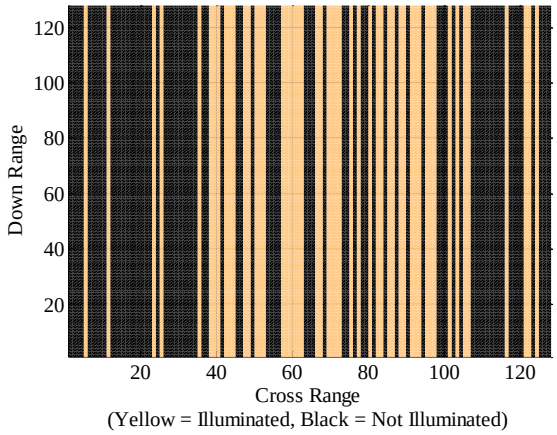

Figure 9. Final VPH for the center cell of the ROI.

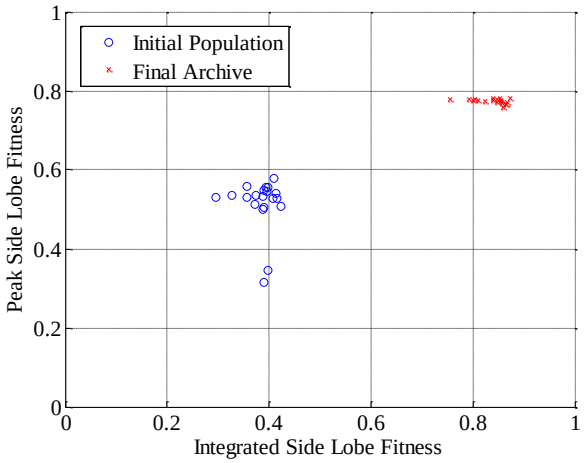

Figure 10. Initial and Final Archive Population Fitness

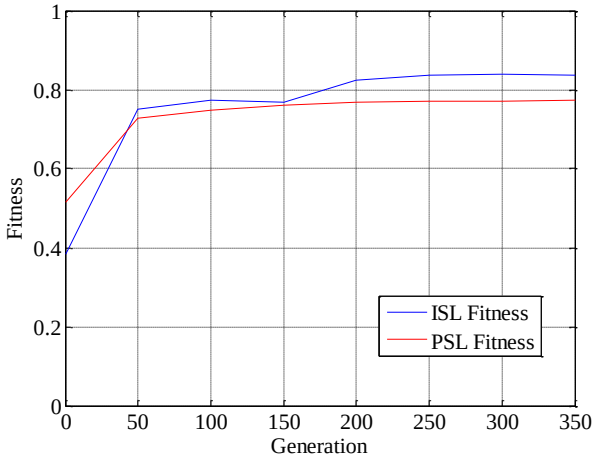

Figure 11. SAR Maximum Member Fitness Improvement

Figure 11 illustrates the rate of change for the ISL and PSL fitness, where ISL continues to improve throughout the generations, while PSL plateaus after 50 generations and sees only marginal (1.5%) improvement.

The performance generated in the simple SAR scenario reproduces the previous [2] work and shows the viability of the new C++ model for improving PSL and ISL.

9. MTI C++ Validation

The purpose of reconstructing the MTI mission in [1] is to baseline the functionality of the new implementation against known results. The scenario parameters in Table 3 are used to run a MTI mission where revisit time and number of pulses are used as the fitness functions in a 3 second run-time scenario.

Table 4. MTI Scenario Parameters

Simulation Parameters	**Value**
No. of Apertures	1
Physical Aperture size	12λ m
Effective aperture length	45 m
Center frequency	600 MHz
Bandwidth	50 MHz
PRF	369 Hz
No. of pulses	1, 8, 16, 32
VPH dimensions	128 x 128
IFFT size	256 x 256
Cross range resolution	3 m
Down range resolution	3 m
Beamwidth	5°
Platform Velocity	130 m/s
Region of Interest Cross Range size	1000 m
Region of Interest Down Range size	45 m
Distance to Region of Interest	500 m
Azimuth angle	-60° to 60° in 32 steps
Objective Functions	Revisit & Pulse Timing
Crossover Operator Uniform	50%
Mutation Operator Binary	5%

The C++ implementation was able to quickly complete the MTI mission and rapidly improved the performance of the archive population members. Comparing against [1] does highlight a discrepancy in the fitness values achieved by the final archive population. Initial random populations for both the original Matlab and new implementation have an average fitness of ~0.5 for both Pulse and Revisit time. After one hundred generations, the Pareto optimal front achieved by the original implementation is at around 0.6 to 0.8. While the new waveform design suite has measured its final archive members to have 0.98 Revisit fitness and 0.9 Pulse fitness. This performance is shown in Figure 12.

This growth is also achieved rapidly; in Figure 6 one can see that the revisit fitness has approached its maximum within 10 generations. When implementing the PSL and ISL calculations for the SAR mission, the original Matlab implementation was directly ported to C++. Pulse fitness however was calculated with a new algorithm and this may explain some of the fitness discrepancy. Originally the pulse fitness was found by calculating the average number of pulses in each ROI cell, then averaging over the total number of ROI cells. The C++ algorithm assigns a fitness value (between 0.0 and 1.0) to each pulses count per CPI type, and then determines how many of each pulse count type occur in a given member. Averaged over the total number of CPI, the summation of the fitness value by the pulse count is used to determine each member's Pulse fitness.

The results of the MTI mission are evolved successfully by the new suite and achieve an even higher performance then the original solution.

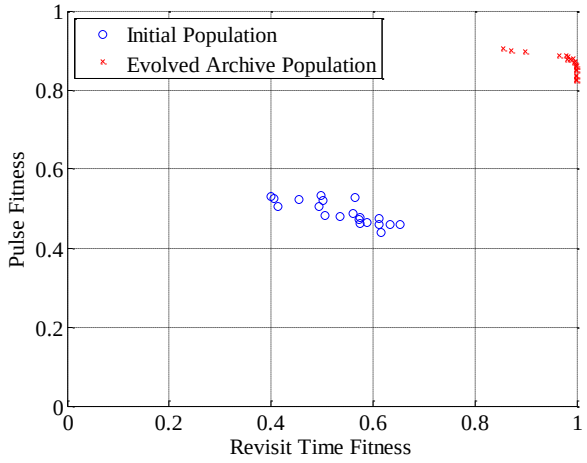

Figure 12. MTI Initial versus Final Archive Fitness (100 Generations)

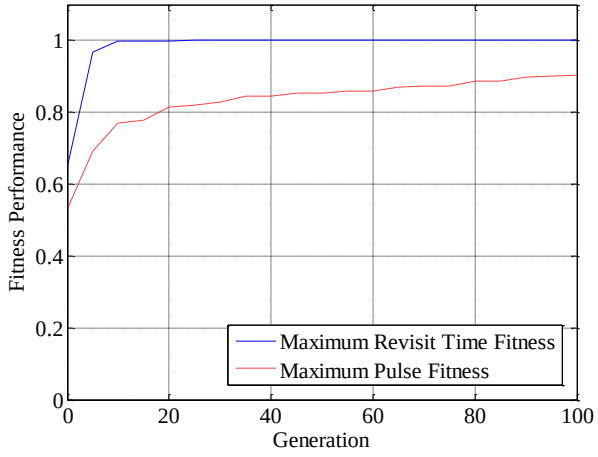

Figure . MTI Maximum Member Fitness Improvement.

10. SAR MPI C++ Validation

Once the MPI extension was completed, the initial small scale SAR scenario was re-executed to validate the distributed algorithm. The parameters were kept identical to the initial SAR scenario, but re-run on the grid system to ensure that similar fitness improvement was observed. The resulting fitness improvement and rate of fitness improvement can be observed in the following figures.

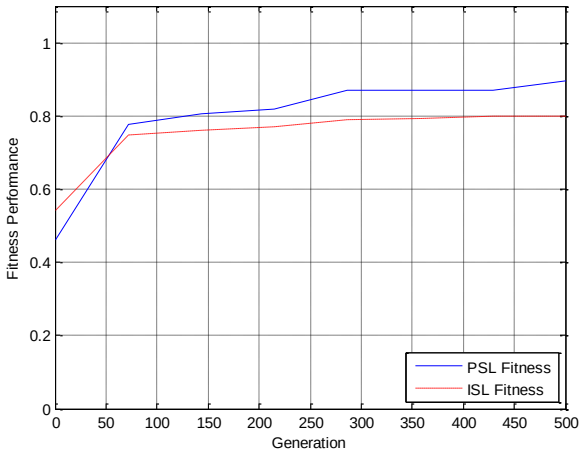

Figure 13. SAR Fitness Improvement per Generation

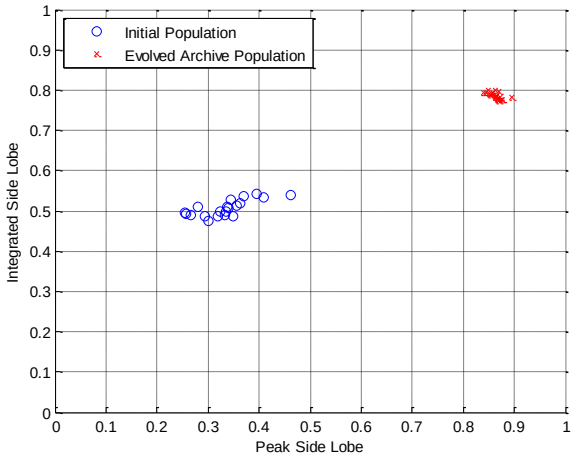

Figure 14. SAR Maximum Member Fitness Improvement

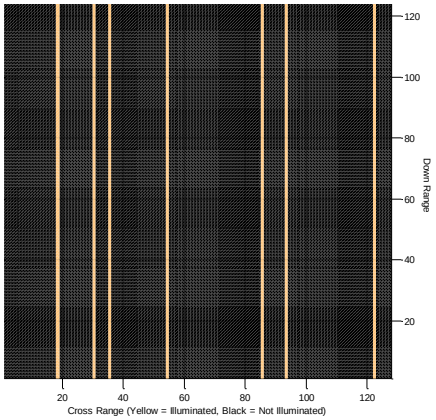

Figure 15. Initial VPH for the center cell of the ROI.

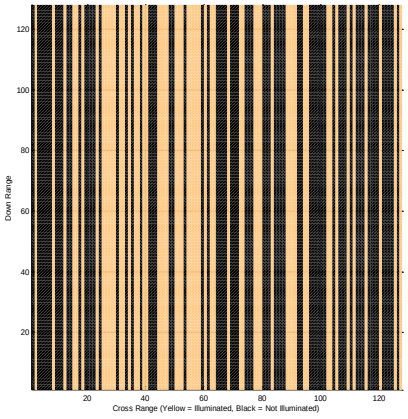

Figure 16. Final VPH for the center cell of the ROI.

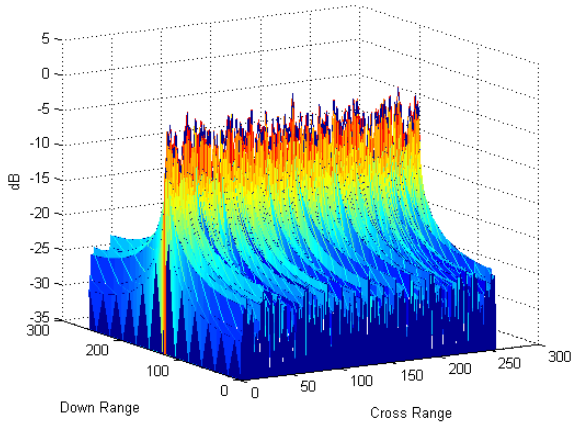

Figure 17. Initial 2D IFFT Normalized Magnitude

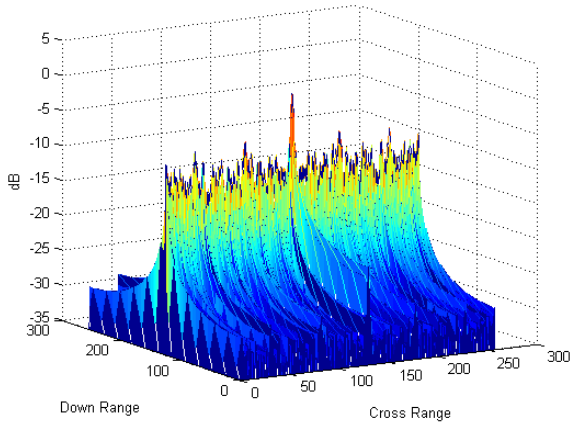

Figure 18. Final 2D IFFT Normalized Magnitude

Performance of the MPI implementation was nearly identical to the gains observed in the single threaded implementation. Figure 8 is the Illuminated VPH for the center cell of an archive member of the randomly generated initial population, while Figure 9 shows the VPH of an archive member from generation 500. There has been a significant improvement (but comparable to the single threaded implementation) in the illumination of the center cell. This yields a significant improvement in PSL and ISL, as can be observed in Figures 10 and 11. The plots show the 2D IFFT magnitudes of generation 0 and generation 500 and one can observe a significantly higher resolution point source in Figure 11.

The improvements in PSL and ISL evident in Figures 17 and 18 correspond to the fitness improvement observed in Figure 7. The PSL and ISL have both improved by 6-7dB, which results in a fitness improvement of .4 for the ISL and .5-.6 for the RSL. This is a comparable level of growth to the initial single threaded implementation, with a small amount of additional improvement achieved in the additional 150 generations the MPI variant was able to run. The growth rate remains front loaded with the greatest improvement in the first 75 generations, but PSL continued to make modest gains for the remainder of the simulation.

11. MTI MPI C++ Validation

This scenario recreates the large MTI scenario, but distributing it with MPI. A 1000m by 45m region of interest was examined over a 3 second simulation evaluating with the revisit time and number of pulses fitness metrics. Now running on the MPI grid, this simulation was able to

be run for 500 generations instead of the 100 used in the Matlab and initial C++ implementations.

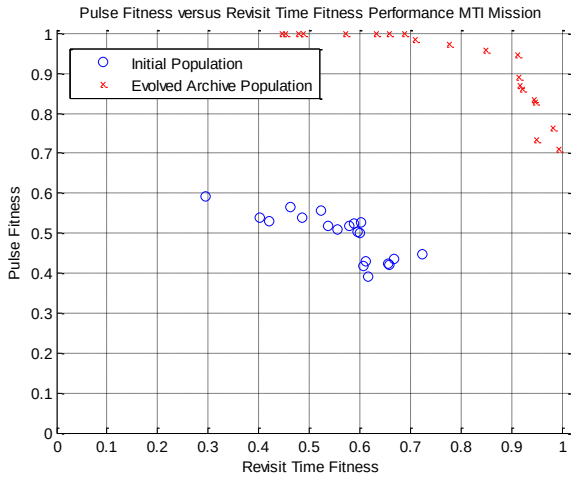

Figure 19. MPI MTI Inivital versus Final Archive Fitness

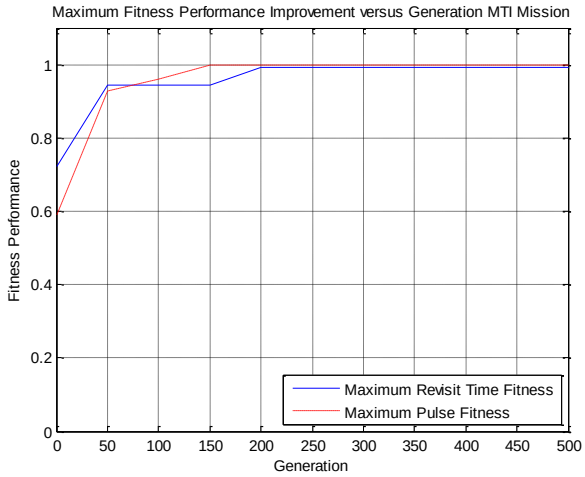

Figure 20. MPI MTI Maximum Member Fitness Improvement

Examining the two figures above one can see a similar level of performance improvement from the initial implementation, when comparing the first 100 generations. The advantage of running for 500 generations appears to be twofold. First, the Pareto Optimal front created by the final archive population covers a wider range of potential solutions, with most of this spread across the Revisit time fitness, but also increased distribution in the Pulse fitness as well. Second, the final improvement of the Pulse fitness has reached the maximum over the course of the run. This simulation validated the ability of the MPI solution to run the MTI scenario accurately and reproduce the previous results.

12. SAR MPI Increased Resolution

In this scenario the same parameters are maintained from the original SAR scenario, except the VPH dimensions and IFFT size are increased. With a VPH dimension of 128 x 256, and scenario time remaining at 0.346 seconds, each CPI illuminates two cross range columns. The IFFT size was increased to 256x512 to retain resolution.

Table 5. SAR Increased Resolution Parameters

Simulation Parameters	**Value**
No. of Apertures	1
Physical Aperture size	12λ m
Effective aperture length	45 m
Center frequency	600 MHz
Bandwidth	50 MHz
PRF	369 Hz
No. of pulses	2
VPH dimensions	128 x 256
IFFT size	256 x512
Cross range resolution	3 m
Down range resolution	3 m
Beamwidth	5°
Platform Velocity	130 m/s
Region of Interest Cross Range size	30 m
Region of Interest Down Range size	45 m
Distance to Region of Interest	500 m
Azimuth angle	-30° to 30° in 32 steps
Objective Functions	Revisit & Pulse Timing
Crossover Operator Uniform	50%
Mutation Operator Binary	5%

The results of this run can be observed in the following Figures where the final improvement of generation 500 is comparable to that of the initial SAR run. PSL fitness has improved from an initial average of 0.47 to 0.90, while ISL has gone from 0.61 to 0.81. The largest discrepancy between the two runs comes from the initial fitness values, while the final are nearly identical. Given the similar convergence point between the two, one must draw the

conclusion that upping the size of the VPH while maintaining the same scenario time yields little benefit to final performance.

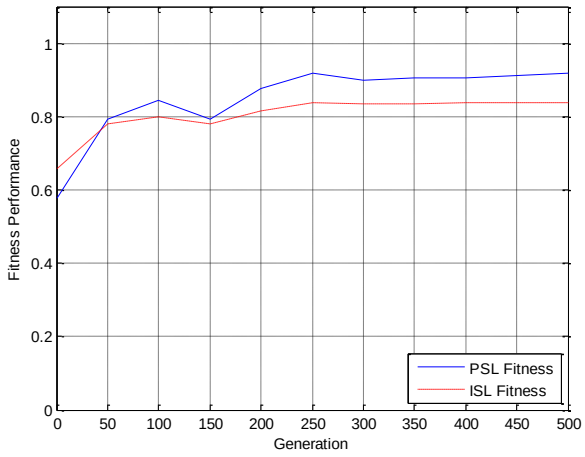

Figure 21. SAR Fitness Improvement per Generation

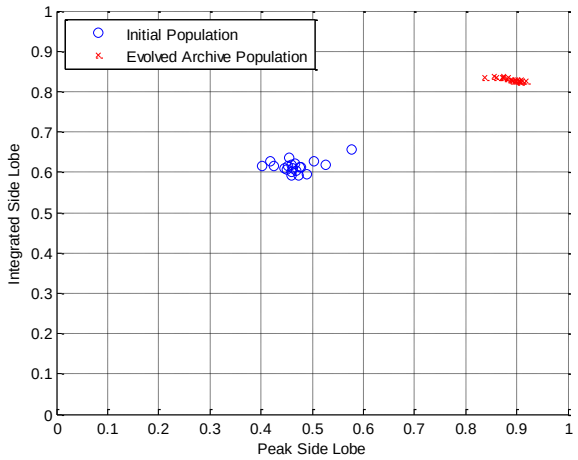

Figure 22. SAR Maximum Member Fitness Improvement

13. SAR MPI Increased ROI Size 45m by 60m

This scenario keeps the increased VPH resolution of the previous solution, but pairs it with an increased scenario ROI and flight time. Increasing the length of the scenario time to 0.692 seconds with the 369 Hz PRF caused each CPI to illuminate one complete cross range column. Doubling the scenario time also allows the target platform to traverse twice the ROI distance during the scenario, increasing the complexity of each population member's genome to twice the number of chromosomes.

Table 6. SAR 45m by 60m Parameters

Simulation Parameters	**Value**
No. of Apertures	1
Physical Aperture size	12λ m
Effective aperture length	45 m
Center frequency	600 MHz
Bandwidth	50 MHz
PRF	369 Hz
No. of pulses	1
VPH dimensions	128 x 256
IFFT size	256 x 512
Cross range resolution	3 m
Down range resolution	3 m
Beamwidth	5°
Platform Velocity	130 m/s
Region of Interest Cross Range size	60 m
Region of Interest Down Range size	45 m
Distance to Region of Interest	500 m
Azimuth angle	-30° to 30° in 32 steps
Objective Functions	Revisit & Pulse Timing
Crossover Operator Uniform	50%
Mutation Operator Binary	5%

Results from this scenario show that configuring the scenario time and PRF such that one CPI illuminates a single cross range column (Figure 25, 26) will produce consistent performance independent of the increase in ROI. Although this required doubling the amount of genetic information, the run-time of this scenario was close to the higher resolution SAR 45m x 30m run. This is due to the fact that most of the processing time is spent in the 2D – IFFT and not determining which VPH bins are illuminated by a particular CPI.

Figures 23 and 24 show the rate of fitness improvement for PSL and ISL and the initial versus final Archive member performance after 500 generations. PSL continues to be the fitness metric most improved by the genetic algorithm, as it starts with a lower fitness and ends higher than the ISL. Initial performance was equivalent to the increased resolution scenario and the

final archive fitness was similar but more tightly grouped. The 500th generation's archive performance also yielded a tight bend with a dense but defined pareto-optimal front emerging. In Figures 27 and 28, one can see the 2 dimensional surface created by the IFFT of the illuminated VPH. Figure 27, from the center ROI cell of an initial population member, has a well defined main lobe, but Figure 28 clearly illustrates the effect of the genetic algorithm. It has improved the performance by roughly 6dB of peak side lobe suppression.

Another way to examine the improvement is to determine whether or not each CPI successfully illuminates at least one pixel of the ROI as defined by the cross and down range resolutions. Figure 29 shows the rate of illumination for a member of the initial and final archive populations. The x-axis is the CPI index and the y-axis is the total number of CPIs whose illumination fell within the ROI. Ideally this would have a slope of 1 and the total number of CPIs would equal the number of hits. Generation zero only yielded 33 ROI hits out of its 256 potential intervals for a success rate of 12.9%. After completion of the algorithm, this has increased to 98 hits or 38.3% hit rate.

This plot allows one to identify, by regions with decreased slope, where the GA could still use improvements. These low increase regions are common in the initial member, but the final archive pushes most of these lower performing regions to the beginning and end of the CPI indices. Given a moving platform that begins and ends at the edge of the ROI, this result is expected as these points in the flight provide the greatest number of Azimuth angles, which can miss the ROI. This information could also yield a more targeted mutation operator in the future. It is also interesting to note that with only 38.3% of the CPIs falling within the region of interest, the population is able to achieve a fitness of 0.88-0.91 in PSL and 0.82 -0.86 ISL, so perhaps the fitness maps could be re-evaluated to achieve greater final scenario performance.

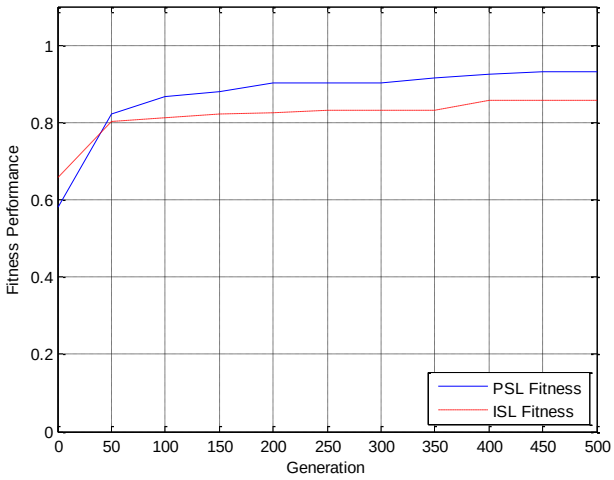

Figure 23. SAR Fitness Improvement per Generation

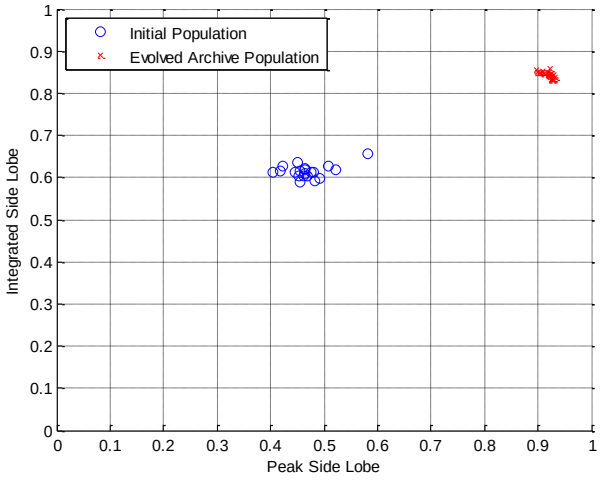

Figure 24. SAR Maximum Member Fitness Improvement

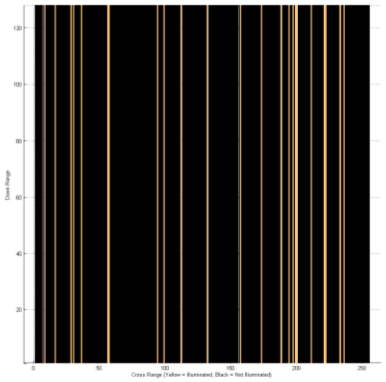

Figure 25.Initial VPH for the center cell of the ROI

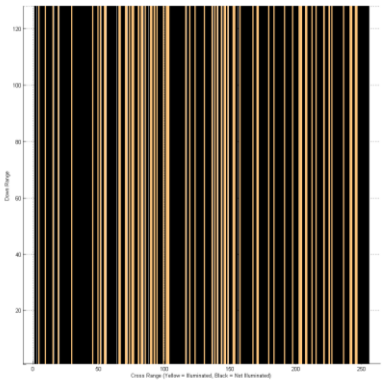

Figure 26. Final VPH for the center cell of the ROI

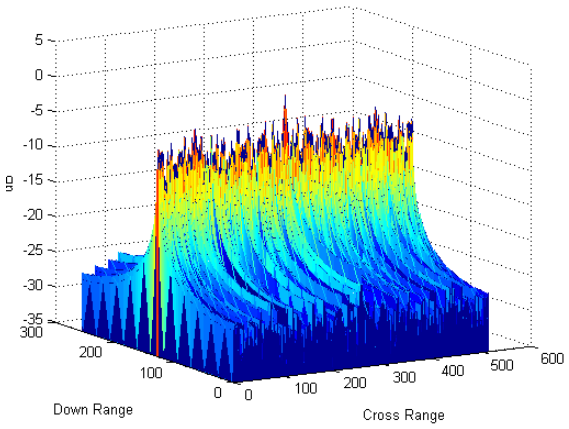

Figure 27. Initial 2D IFFT Normalized Magnitude

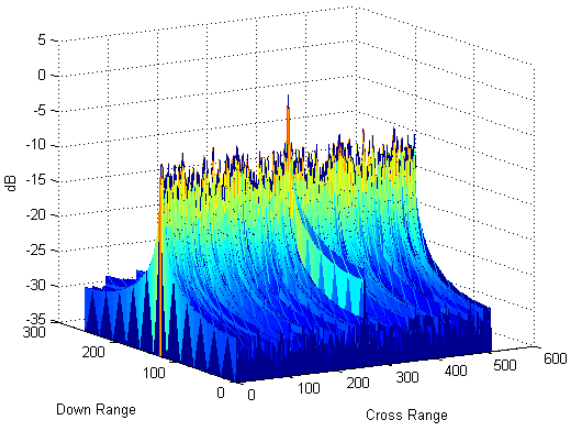

Figure 28. Final 2D IFFT Normalized Magnitude

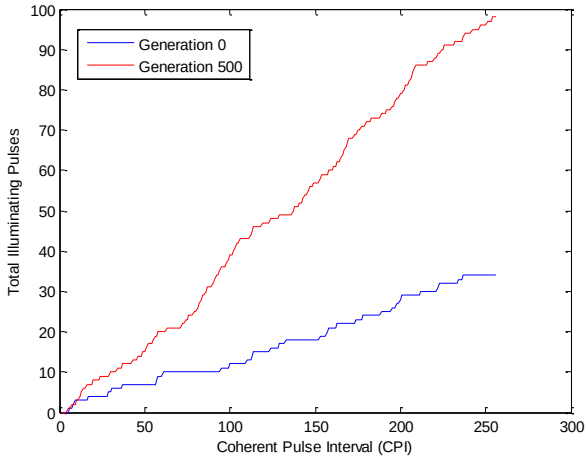

Figure 29. ROI Illumination per CPI

14. SAR MPI Scenario 45m by 120m

Maintaining a similar computational burden to the previous simulations, a larger ROI of 120m in the cross range dimension was examined. A simulation time of 1.384 and a PRF of 369 achieved a single cross range column illumination by upping the pulses per CPI to two from the single pulse used in all preceding scenarios.

Table 7. SAR 45m by 120m Parameters

Simulation Parameters	**Value**
No. of Apertures	1
Physical Aperture size	12λ m
Effective aperture length	45 m
Center frequency	600 MHz
Bandwidth	50 MHz
PRF	369 Hz
No. of pulses	2
VPH dimensions	128 x 256
IFFT size	256 x 512
Cross range resolution	3 m
Down range resolution	3 m
Beamwidth	5°
Platform Velocity	130 m/s
Region of Interest Cross Range size	120 m
Region of Interest Down Range size	45 m
Distance to Region of Interest	500 m
Azimuth angle	-31° to 31° in 32 steps
Objective Functions	Revisit & Pulse Timing
Crossover Operator Uniform	50%
Mutation Operator Binary	5%

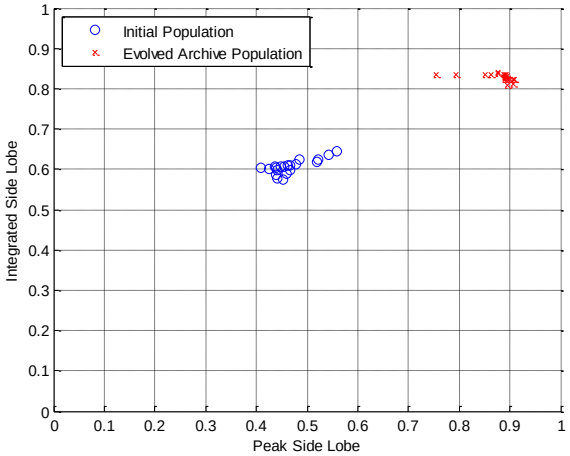

Figure 30. SAR Fitness Improvement per Generation

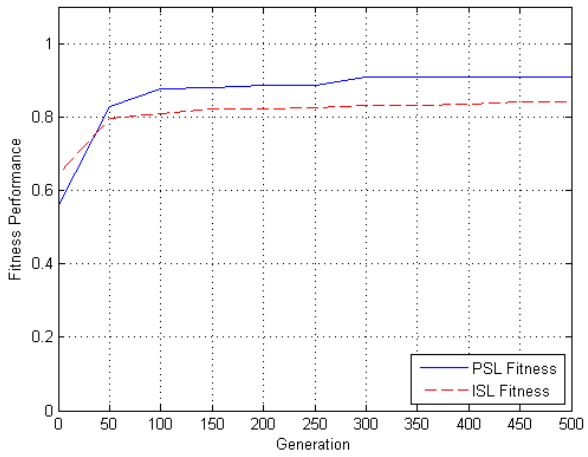

Figure 31. SAR Maximum Member Fitness Improvement

Figures 30 and 31 show that this scenario configuration experienced results consistent with the previous experiments. PSL initially starting with a lower performance was rapidly improved to an average fitness of 0.9 and ISL improved to 0.88. Examining the VPH and IFFT's for the center cell also reinforced that when constrained to the same illumination per CPI, the results are similar despite changes to the scenario time and ROI length.

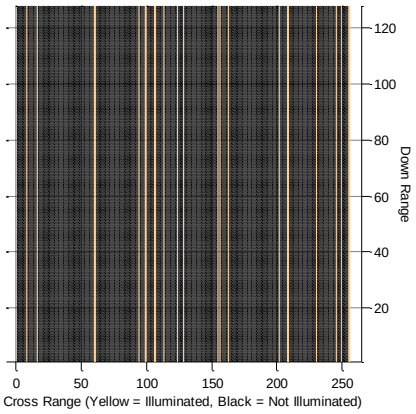

Figure 32. Initial VPH for the center cell of the ROI

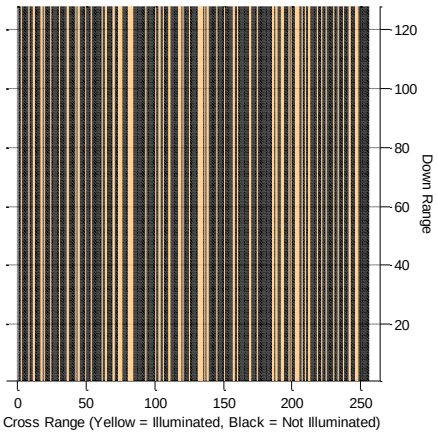

33. Final VPH for the center cell of the ROI.

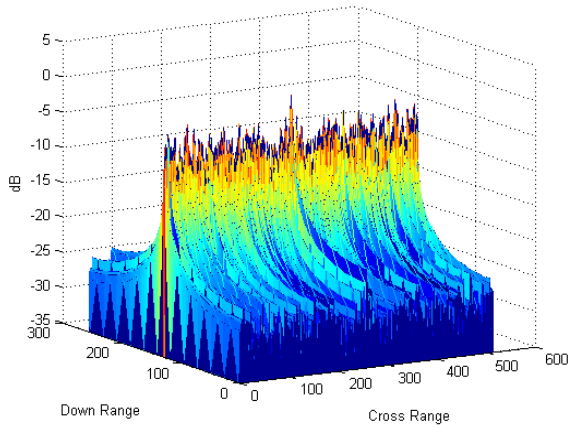

Figure 34. Initial 2D IFFT Normalized Magnitude

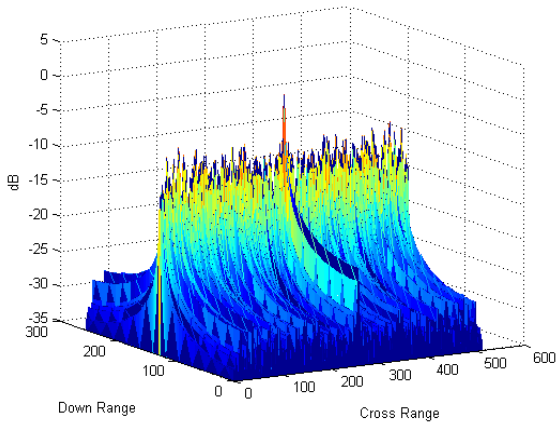

Figure 35. Final 2D IFFT Normalized Magnitude

15. SAR 45m by 60m with 4 Apertures

This scenario is the first to utilize multiple sub-apertures and apply them to a ROI of 45m by 60m. With the exception of the sub-apertures, the scenario is identical to section 14, running for 0.692 seconds with a VPH size of 128 by 256. This run time allows the target platform to traverse the length of the 60m ROI. Each CPI sub-aperture is allocated 12.5 MHz, or one quarter of the down range resolution (32 cells), and one column in the cross range dimension. This allocation of bandwidth yields VPH illumination patterns that are no longer symmetrical about the center of the down range dimension and can be observed in Figures 38 and 39.

Table 8. SAR 45m by 60m with 4 Aperutres Parameters

Simulation Parameters	**Value**
No. of Apertures	4
Physical Aperture size	12λ m
Effective aperture length	45 m
Center frequency	600 MHz
Bandwidth	50 MHz
PRF	369 Hz
No. of pulses	1
VPH dimensions	128 x 256
IFFT size	256 x 512
Cross range resolution	3 m
Down range resolution	3 m
Beamwidth	5°
Platform Velocity	130 m/s
Region of Interest Cross Range size	60 m
Region of Interest Down Range size	45 m
Distance to Region of Interest	500 m
Azimuth angle	-30° to 30° in 32 steps
Objective Functions	Revisit & Pulse Timing
Crossover Operator Uniform	50%
Mutation Operator Binary	5%

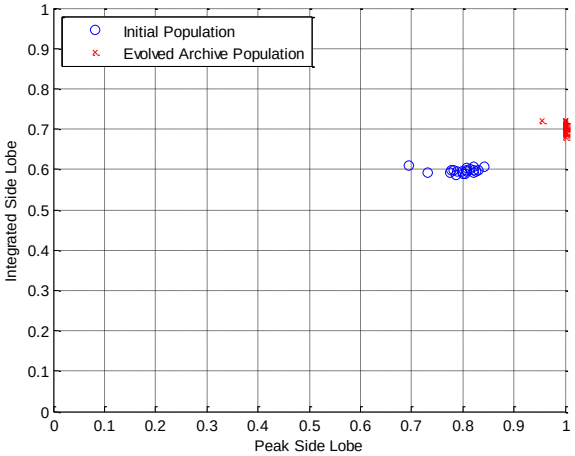

Figure 36. SAR Fitness Improvement per Generation

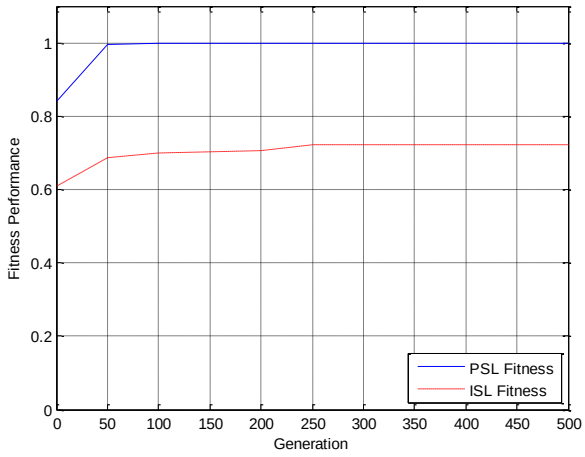

Figure 37. SAR Maximum Member Fitness Improvement

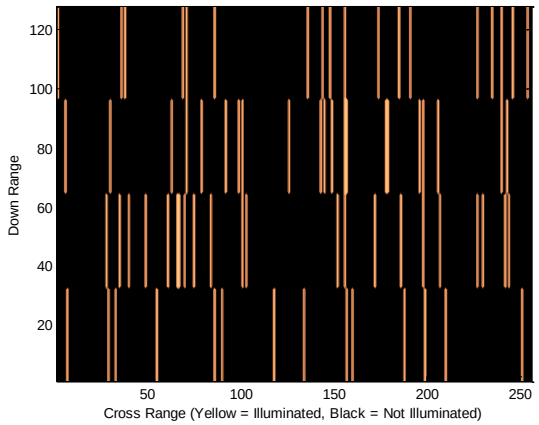

Figure 38. Initial VPH for the center cell of the ROI

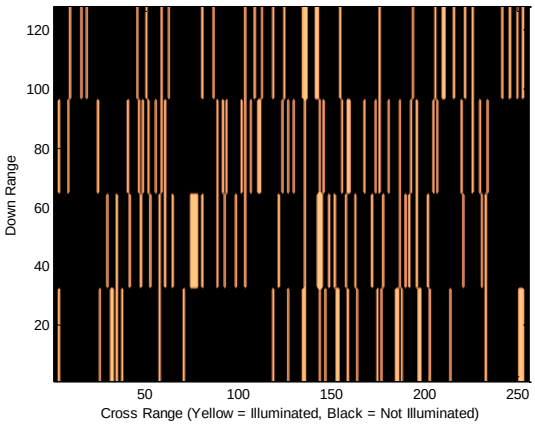

Figure 39. Final VPH for the center cell of the ROI

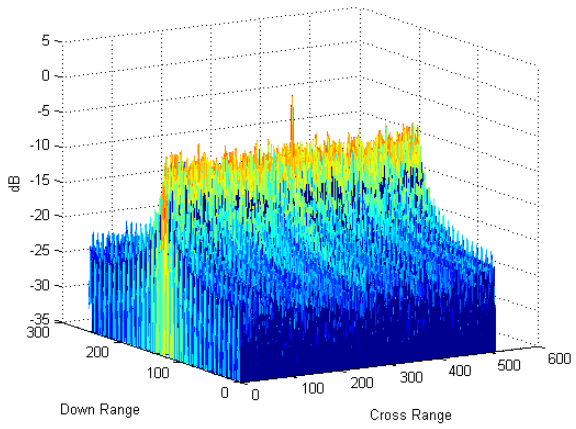

Figure 40. Initial 2D IFFT Normalized Magnitude

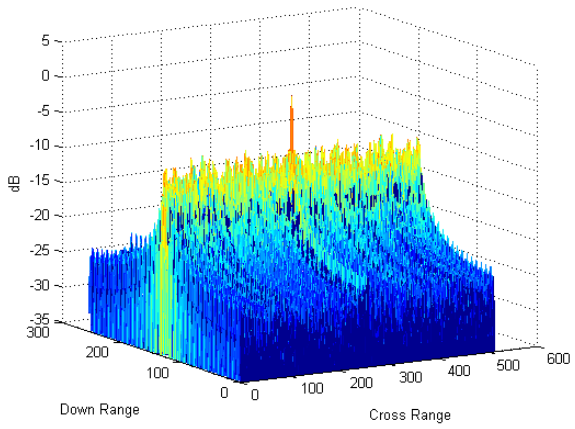

Figure 41. Final 2D IFFT Normalized Magnitude

The results from this scenario offered a significant departure from the previous simulations. Initial ISL performance shown in Figure 36, was comparable to the results in section 14, starting with a fitness value of 0.6. PSL, which previously began lower then ISL, found an initial value of 0.8, which was well above the expected ~0.48 fitness. One can see in Figure 37 that PSL performance rocketed to saturation by the 50^{th} generation, while the ISL only managed to gain ~0.1 for a final archive fitness 0.7.

Comparing against previous sub-aperture work [1], one can see that this PSL and ISL tradeoff is the anticipated result of introducing multiple sub-apertures. This simulation reinforces the rapid improvement in PSL that can be achieved at the cost of ISL performance. Further investigation should target whether the saturation of PSL fitness prevents further growth in the ISL dimension. A new fitness map for the PSL function would also allow for one to determine the maximum achievable PSL dB value, as the members in this simulation were not rewarded for performance beyond the 14dB value seen in Figure 41.

16. <u>SAR 45m by 1000m</u>

This scenario is an attempt at running the SAR optimization on a ROI with the dimensions used for the MTI mission. The cross range ROI size was increased to 1000 meters and the scenario run time was set to 7.6293 seconds to allow the platform to fully traverse the ROI. Instead of a -30° to 30° Azimuth angle, the genetic algorithm was set to optimize for values between -60° and 60°. PRF was increased to 530 Hz, but the number of pulses per CPI was increased to 16 to yield a CR illumination of one column per CPI.

Table 9. SAR 45m by 1000m Parameters

Simulation Parameters	Value
No. of Apertures	1
Physical Aperture size	12λ m
Effective aperture length	45 m
Center frequency	600 MHz
Bandwidth	50 MHz
PRF	530 Hz
No. of pulses	16
VPH dimensions	128 x 256
IFFT size	256 x 512
Cross range resolution	3 m
Down range resolution	3 m
Beamwidth	5°
Platform Velocity	130 m/s
Region of Interest Cross Range size	1000 m
Region of Interest Down Range size	45 m
Distance to Region of Interest	500 m
Azimuth angle	-60° to 60° in 32 steps
Objective Functions	Revisit & Pulse Timing
Crossover Operator Uniform	50%
Mutation Operator Binary	5%

Based on the results of the previous experiments, one would have expected similar performance of the PSL and ISL as each CPI is again illuminating a single cross-range column. Although this scenario was only run for 300 generations versus the 500 of the pervious simulations, both the initial and final fitness proved to be lower than expected.

One can see in Figure 43, initial PSL performance fell from a fitness of 0.6 to 0.36, almost a 50% falloff compared to the 45m by 120m scenario. ISL also dropped to 0.59 from a typical start of ~0.63. This starting deficiency was compounded by reduced performance improvement across all generations of the scenario. Figure 42 shows that while PSL improved by ~0.3 in the smaller scenarios, here it only experienced 0.1 fitness growth over the course of its 300 generations. ISL improvement, which has consistently underperformed PSL in previous

scenarios, was even slow to improve. ISL only gains 0.05 fitness in this 1000m scenario, which is half the performance of the 120m scenario. One can see the small improvement between Figure 44 and Figure 45; this cell has only gained a small amount of illumination after the 300 generations have run their course.

This scenario baselines the SAR performance in a large scale scenario so that it can be compared against the large combined SAR/MTI mission, as well as combined with multiple sub-aperture missions. Performance would likely be improved by tweaking the pulse per CPI, PRF and CR VPH resolution parameters.

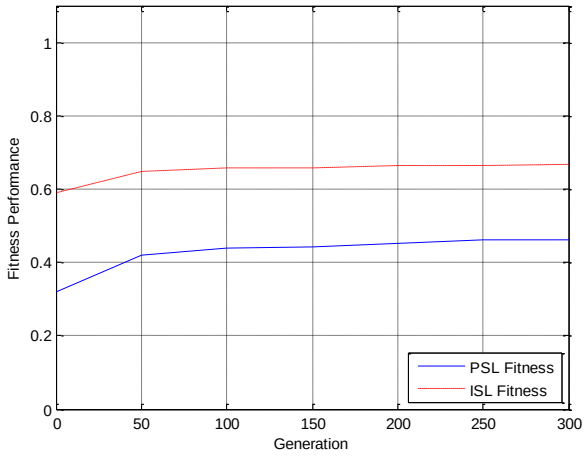

Figure 42. SAR Fitness Improvement per Generation

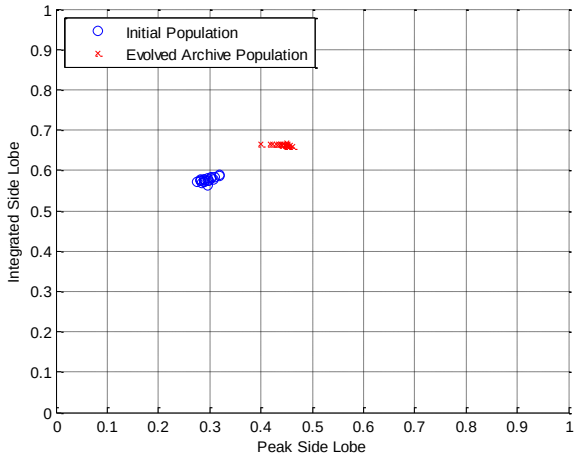

Figure 43. SAR Maximum Member Fitness Improvement

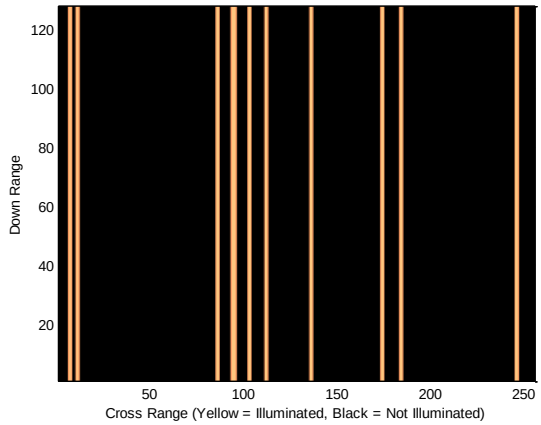

Figure 44. Initial VPH for the center cell of the ROI

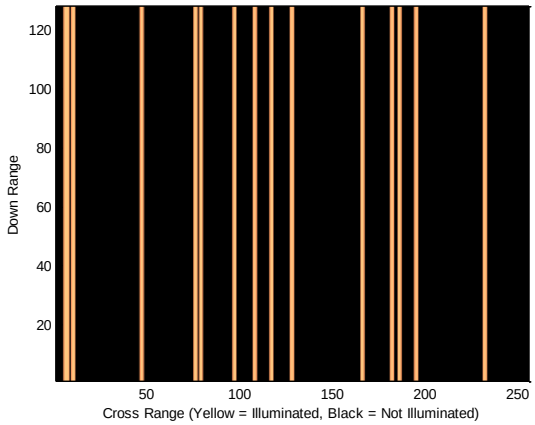

Figure 45. Final VPH for the center cell of the ROI

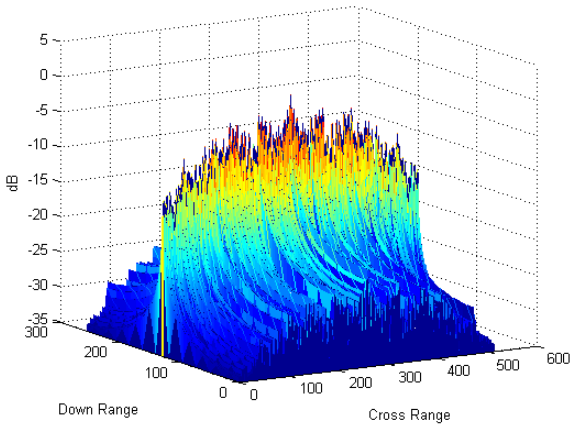

Figure 46. Initial 2D IFFT Normalized Magnitude

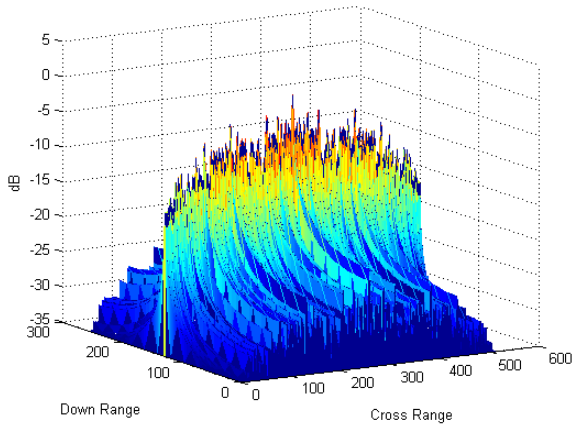

Figure 47. Final 2D IFFT Normalized Magnitude

17. SAR & MTI 45m by 1000m

This scenario combines the SAR and MTI missions for a 4-dimensional SPEA2 optimization run. It uses 2 dynamic parameters encoded into each CPI, the number of pulses and the angle from -60° to 60°. The combination of a simultaneous SAR and MTI mission, as well as running a SAR mission with a SPEA2 driven number of pulses were both novel to this scenario. The dynamic pulse number was required as it is a crucial part of the fitness metrics used for the MTI mission.

Table 10. SAR and MTI Parameters

Simulation Parameters	**Value**
No. of Apertures	1
Physical Aperture size	12λ m
Effective aperture length	45 m
Center frequency	600 MHz
Bandwidth	50 MHz
PRF	369 Hz
No. of pulses	1, 8, 16, 32
VPH dimensions	128 x 256
IFFT size	256 x 512
Cross range resolution	3 m
Down range resolution	3 m
Beamwidth	5°
Platform Velocity	130 m/s
Region of Interest Cross Range size	1000 m
Region of Interest Down Range size	30 m
Distance to Region of Interest	500 m
Azimuth angle	-60° to 60° in 32 steps
Objective Functions	Revisit & Pulse Timing
Crossover Operator Uniform	50%
Mutation Operator Binary	5%

Unfortunately, the addition of the MTI mission did not provide any benefit to the SAR mission when comparing against the pervious scenario. Initial ISL and PSL performance was equivalent with 0.59 and 0.37, respectively. Fitness growth across the 500 generations was weak even when compared to the results of the previous 1000m SAR scenario. PSL and ISL both grew by ~0.04; a very marginal improvement.

The MTI fitness metrics performed differently from the expectations set by the previous stand-alone run. Revisit time increased its initial starting value from 0.7 to ~0.9, while Pulse fitness fell from 0.6 to 0.5. The revisit time fitness was able to reach saturation, as it did in the prior run, but the maximum pulse fitness was held to 0.7, a gain of 0.2. Looking at Figure 51,

one can see that the pareto-optimal front was not the clean band previously observed in the MTI mission. The diffusion is likely a result of now optimizing across the 4 fitness function.

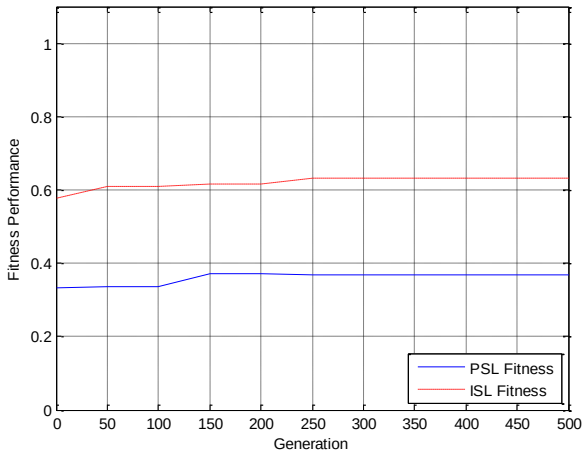

Figure 48. SAR Fitness Improvement per Generation

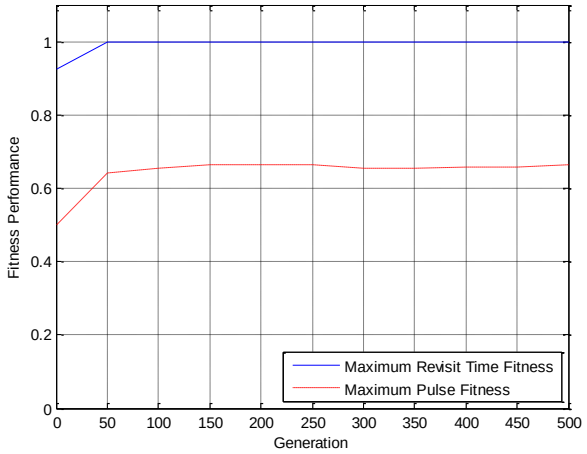

Figure 49. MTI Fitness Improvement per Generation

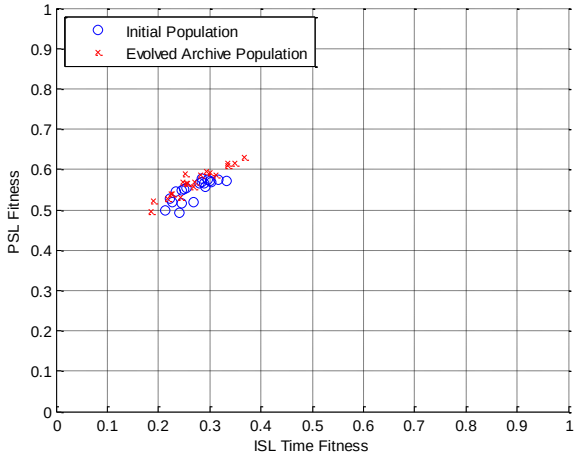

Figure 50. SAR Maximum Member Fitness Improvement

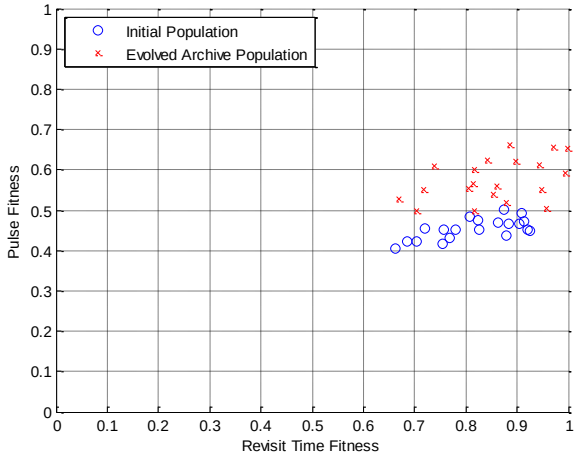

Figure 51. MTI Maximum Member Fitness Improvement

18. SAR & MTI 45m by 1000m 4 Apertures

This scenario combines all the previous investigations to produce a waveform controlling 4 sub-apertures across a 7.6293 second scenario. The algorithm is run with both the SAR and MTI fitness functions for 500 generations.

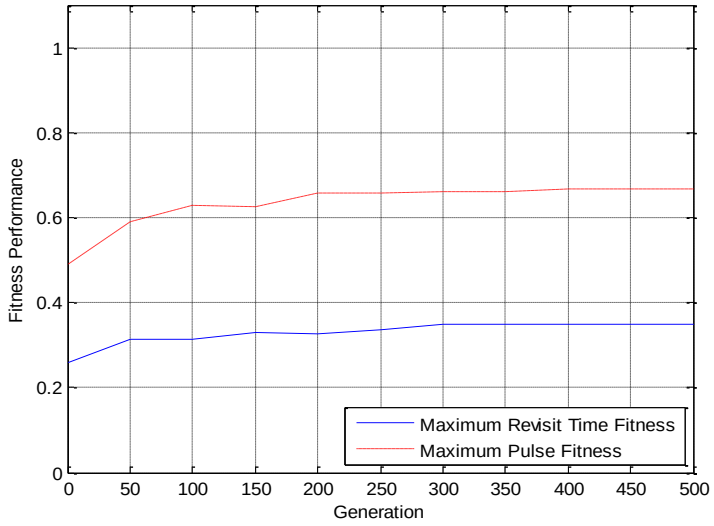

Figure 52. SAR Fitness Improvement per Generation

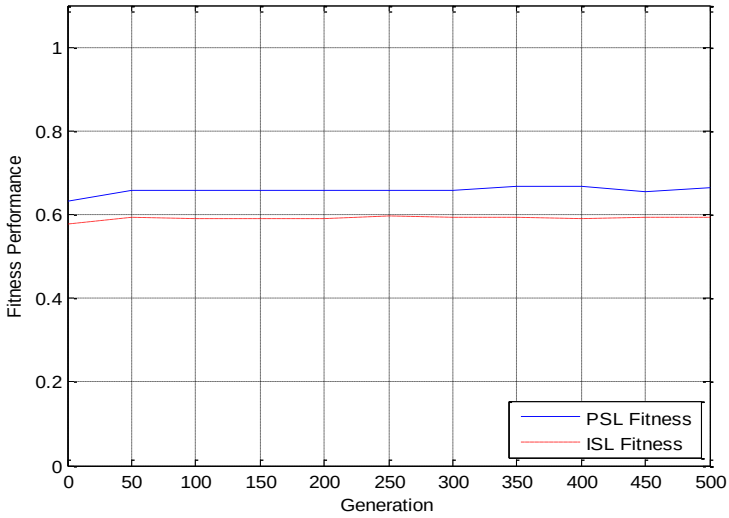

Figure 53. MTI Fitness Improvement per Generation

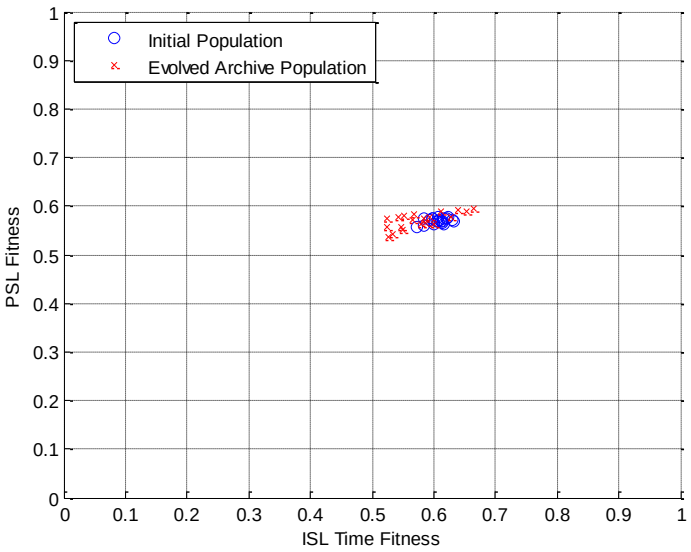

Figure 54. SAR Maximum Member Fitness Improvement

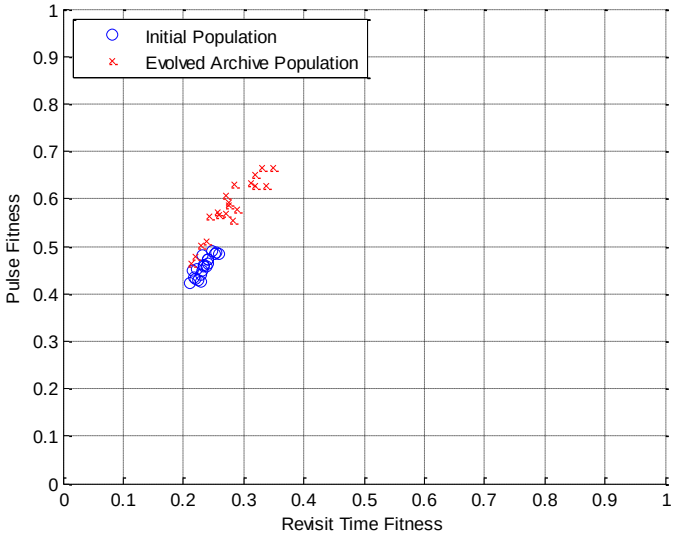

Figure 55. MTI Maximum Member Fitness Improvement

As one can see from the above figures, the performance of this simulation was again not ideal. Adding sub-apertures to the MTI mission greatly reduced the performance of both the revisit time and the pulse fitness. The apertures did improve the initial PSL and ISL values, as with the previous scenarios, where they were introduced and all other parameters kept the same. Despite this, they provided barely any improvement over the 500 iterations, gaining ~0.02 fitness. The revisit time and pulse fitness gained 0.2 and 0.08, a more significant delta, but still

small when compared against the independent scenarios. One can notice a very small improvement in illumination when comparing Figures 56 and 57.

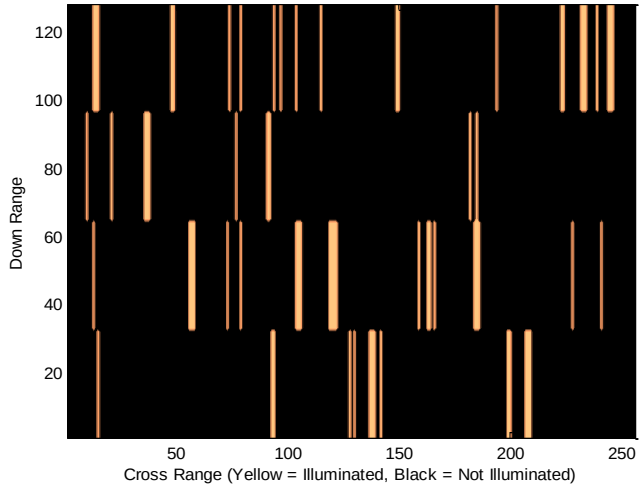

Figure 56. Initial VPH for the center cell of the ROI

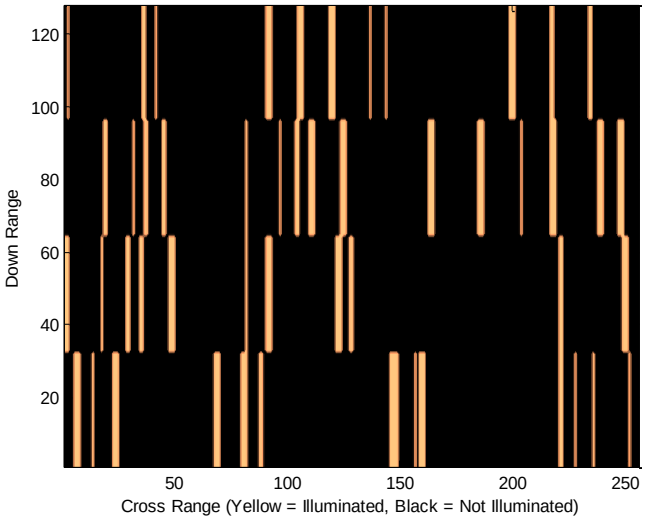

Figure 57. Final VPH for the center cell of the ROI

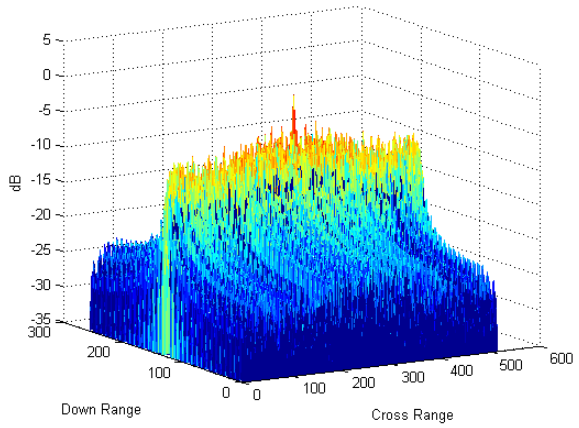

Figure 58. Initial 2D IFFT Normalized Magnitude

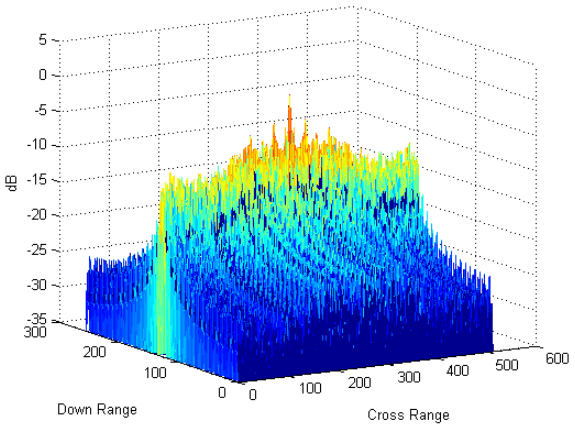

Figure 59. Final 2D IFFT Normalized Magnitude

19. Conclusion

These initial simulation results validate the C++ model of SPEA2 and the multi-mission radar waveform design suite by successfully reproducing the results of the previous Matlab version. The new implementation has provided a computational efficiency boost, even when running on a single processing core, which has allowed testing of simultaneous MTI and SAR missions.

Aside from the run-time performance gained by transitioning to C++, this new waveform design suite was run on a multi-core grid computer to examine even more realistic scenarios. Distributing the SPEA2 algorithm across a grid using MPI allowed for multiple population members to be examined in parallel. This allowed for scenarios involving 256 by 512 2-D IFFTs to complete within a fraction of the time required for the original Matlab implementation. Multiple experiments proved that various parameters could be adjusted and the results would scale as anticipated.

The initial combined runs of SAR and MTI missions proved disappointing in both initial fitness and growth over the generations. This will prove a useful area for further investigation, to determine if higher resolution, especially in the cross-range, can allow for more successful solutions.

Another area of future research would be into alternative fitness metrics, especially for SAR's PSL and ISL. Given that the fitness is tightly coupled to the total illumination of VPH, a rough fitness metric could be gained without computing the full IFFT. This would allow for further reduction in run-time, reserving the high-cost PSL and ISL functions for later generations or specific portions of the ROI.

20. Citations

[1] Jason W. Enslin, "An Evolutionary Algorithm Approach to Simultaneous Multi-Mission Radar Waveform Design," Department of Electrical Engineering, Rochester Institute of Technology, August 2007, Rochester, New York.

[2] V.J. Amuso and J. Enslin, "The Strength Pareto Evolutionary Algorithm 2 Applied to Simultaneous Multi-mission Waveform Design," Third International Conference on Waveform Diversity and Design, June 2007, Pisa, Italy.

[3] E. Zitzler, M. Laumanns, and L. Thiele, "SPEA2: Improving the Strength Pareto Evolutionary Algorithm for Multiobjective Optimization," Evolutionary Methods for Design, Optimization and Control with Application to Industrial Problems (EUROGEN 2001), K.C. Giannakoglou et al. (ED), International Center for Numerical Methods in Engineering, 2002, pp.95-100

[4] M.L. Skolnik, Introduction to Radar Systems, Mcgraw-Hill, St. Louis, 1980

[5] B. Wilkinson and Michael Allen, Parallel Programming Techniques and Applications using Networked Workstations and Parallel Computers, Prentice Hall, Upper Saddle River, New Jersey, 1999

[6] V.J. Amuso, P. Antonik, R. Schneible, Y. Zhang, Evolutionary Computation Approach to Multi Mission Waveform Design, RADAR 2002, Edinburgh, UK, October 2002, pp. 454-458.

[7] V.J. Amuso, P. Antonik, R. Schneible, Y. Zhang, A Strength Pareto Evolutionary Algorithm (SPEA) for Multi-Mission Radar Waveform Optimization, First International Conference on Waveform Diversity and Design, November 2004, Edinburgh, UK.

[8] C. M. Fonseca and P. J. Fleming, "An overview of evolutionary algorithms in multiobjective optimization," Evol. Comput., vol. 3, no. 1, pp. 1–16, 1995.

[9] Bleuler, S.; Brack, M.; Thiele, L.; Zitzler, E., " Multiobjective genetic programming: reducing bloat using SPEA2," Evolutionary Computation, 2001 536 - 543 vol. 1.

[10] Tse Guan Tan Hui Keng Lau Teo, J., "Cooperative Coevolution for Pareto Multiobjective Optimization: An Empirical Study using SPEA2," TENCON 2007 - 2007 IEEE Region 10 Conference , Oct. 30 2007-Nov. 2 2007.

[11] Eckart Zitzler and Lothar Thiele, "Multiobjective Evolutionary Algorithms:A Comparative Case Study andthe Strength Pareto Approach," IEEE Transactions on Evolutionary Computation, VOL. 3, NO. 4, NOVEMBER 1999 257.

[12] D.S. Weile and E. Michielssen, "Genetic Algorithm Optimization Applied to Electromagnetics: A Review," IEEE Transactions on Antennas and Propagation, Vol. 45, No. 3, March 1997, pp. 343-353.

[13] Bjarne Stroustrup, The C++ Programming Language, Addison-Wesley, August 2004.

[14] Erich Gamma, Richard Helm, Ralph Johnson, John Vlissides, Design Patterns: Elements of Reusable Object-Oriented Software , 10 November 1994.

[15] FFTW Library 3.3, http://www.fftw.org/

[16] MPI Documentation, http://www.open-mpi.org/doc/v1.4/

[17] GNU GCC compiler, http://gcc.gnu.org/